



Highly Abrasion-resistant and Long-lasting Concrete



Prall samples after testing (Bowthorpe, 2019)

Prepared by:

Jenny Liu, Ph.D. and Diane Murph

Report # FHWA-AK-RD-4000(177)

August 2019

Prepared for:

Alaska Department of Transportation & Public Facilities
Statewide Research Office
3132 Channel Drive
Juneau, AK 99801-7898

Alaska Department of Transportation & Public Facilities

Research & Technology Transfer

REPORT DOCUMENTATION PAGE

Form approved OMB No.

Public reporting for this collection of information is estimated to average 1 hour per response, including the time for reviewing instructions, searching existing data sources, gathering and maintaining the data needed, and completing and reviewing the collection of information. Send comments regarding this burden estimate or any other aspect of this collection of information, including suggestion for reducing this burden to Washington Headquarters Services, Directorate for Information Operations and Reports, 1215 Jefferson Davis Highway, Suite 1204, Arlington, VA 22202-4302, and to the Office of Management and Budget, Paperwork Reduction Project (0704-1833), Washington, DC 20503

1. AGENCY USE ONLY (LEAVE BLANK)

2. REPORT DATE

3. REPORT TYPE AND DATES COVERED

08/2019

Final Report: 01/2017 – 08/2019

4. TITLE AND SUBTITLE

Highly Abrasion-resistant and Long-lasting Concrete

5. FUNDING NUMBERS

CESTiCC 1617

6. AUTHOR(S)

Jenny Liu and Diane Murph

7. PERFORMING ORGANIZATION NAME(S) AND ADDRESS(ES)

Department of Civil, Architectural, and Environmental Engineering
 Missouri University of Science and Technology
 Rolla, MO 65409

8. PERFORMING ORGANIZATION REPORT NUMBER

INE/CESTiCC 19.21

9. SPONSORING/MONITORING AGENCY NAME(S) AND ADDRESS(ES)

Center for Environmentally Sustainable Transportation in Cold Climates
 University of Alaska Fairbanks
 P.O. Box 755900
 Fairbanks, AK 99775-5900

10. SPONSORING/MONITORING AGENCY REPORT NUMBER

Alaska DOT&PF HFHWY00080
 FHWA-AK-RD-4000 (177)

Alaska Department of Transportation & Public Facilities Statewide Research Office
 3132 Channel Drive
 Juneau, AK 99801-7898

11. SUPPLEMENTARY NOTES

12a. DISTRIBUTION / AVAILABILITY STATEMENT

No restrictions

12b. DISTRIBUTION CODE

13. ABSTRACT (Maximum 200 words)

Studded tire usage in Alaska contributes to rutting damage on pavements resulting in high maintenance costs and safety issues. In this study binary, ternary, and quaternary highly-abrasion resistant concrete mix designs, using supplementary cementitious materials (SCMs), were developed. The fresh, mechanical and durability properties of these mix designs were then tested to determine an optimum highly-abrasion resistant concrete mix that could be placed in cold climates to reduce rutting damage. SCMs used included silica fume, ground granulated blast furnace slag, and type F fly ash. Tests conducted measured workability, air content, drying shrinkage, compressive strength, flexural strength, and chloride ion permeability. Resistance to freeze-thaw cycles, scaling due to deicers, and abrasion resistance were also measured. A survey and literature review on concrete pavement practices in Alaska and other cold climates was also conducted. A preliminary construction cost analysis comparing the concrete mix designs developed was also completed.

14- KEYWORDS : Abrasion, Cold Climate Concrete, Freeze-thaw, Supplementary Cementitious Materials (SCMs), Cost Analysis

15. NUMBER OF PAGES

119

16. PRICE CODE

N/A

17. SECURITY CLASSIFICATION OF REPORT

Unclassified

18. SECURITY CLASSIFICATION OF THIS PAGE

Unclassified

19. SECURITY CLASSIFICATION OF ABSTRACT

Unclassified

20. LIMITATION OF ABSTRACT

N/A

**HIGHLY ABRASION-RESISTANT AND LONG-LASTING
CONCRETE**

FINAL REPORT

Prepared for

**Center for Environmentally Sustainable Transportation in Cold
Climates**

and

Alaska Department of Transportation & Public Facilities

Authors:

Jenny Liu, Ph.D., P.E.

Diane Murph

Missouri University of Science and Technology

August 2019

DISCLAIMER

This document is disseminated under the sponsorship of the U. S. Department of Transportation in the interest of information exchange. The U.S. Government assumes no liability for the use of the information contained in this document. The U.S. Government does not endorse products or manufacturers. Trademarks or manufacturers' names appear in this report only because they are considered essential to the objective of the document.

METRIC (SI*) CONVERSION FACTORS

APPROXIMATE CONVERSIONS TO SI UNITS					APPROXIMATE CONVERSIONS FROM SI UNITS																				
Symbol	When You Know	Multiply By	To Find	Symbol	Symbol	When You Know	Multiply By	To Find	Symbol																
<u>LENGTH</u>					<u>LENGTH</u>																				
in	inches	25.4		mm	mm	millimeters	0.039	inches	in																
ft	feet	0.3048		m	m	meters	3.28	feet	ft																
yd	yards	0.914		m	m	meters	1.09	yards	yd																
mi	Miles (statute)	1.61		km	km	kilometers	0.621	Miles (statute)	mi																
<u>AREA</u>					<u>AREA</u>																				
in ²	square inches	645.2	millimeters squared	cm ²	mm ²	millimeters squared	0.0016	square inches	in ²																
ft ²	square feet	0.0929	meters squared	m ²	m ²	meters squared	10.764	square feet	ft ²																
yd ²	square yards	0.836	meters squared	m ²	km ²	kilometers squared	0.39	square miles	mi ²																
mi ²	square miles	2.59	kilometers squared	km ²	ha	hectares (10,000 m ²)	2.471	acres	ac																
ac	acres	0.4046	hectares	ha																					
<u>MASS (weight)</u>					<u>MASS (weight)</u>																				
oz	Ounces (avdp)	28.35	grams	g	g	grams	0.0353	Ounces (avdp)	oz																
lb	Pounds (avdp)	0.454	kilograms	kg	kg	kilograms	2.205	Pounds (avdp)	lb																
T	Short tons (2000 lb)	0.907	megagrams	mg	mg	megagrams (1000 kg)	1.103	short tons	T																
<u>VOLUME</u>					<u>VOLUME</u>																				
fl oz	fluid ounces (US)	29.57	milliliters	mL	mL	milliliters	0.034	fluid ounces (US)	fl oz																
gal	Gallons (liq)	3.785	liters	liters	liters	liters	0.264	Gallons (liq)	gal																
ft ³	cubic feet	0.0283	meters cubed	m ³	m ³	meters cubed	35.315	cubic feet	ft ³																
yd ³	cubic yards	0.765	meters cubed	m ³	m ³	meters cubed	1.308	cubic yards	yd ³																
Note: Volumes greater than 1000 L shall be shown in m ³																									
<u>TEMPERATURE (exact)</u>					<u>TEMPERATURE (exact)</u>																				
°F	Fahrenheit temperature	5/9 (°F-32)	Celsius temperature	°C	°C	Celsius temperature	9/5 °C+32	Fahrenheit temperature	°F																
<u>ILLUMINATION</u>					<u>ILLUMINATION</u>																				
fc	Foot-candles	10.76	lux	lx	lx	lux	0.0929	foot-candles	fc																
fl	foot-lamberts	3.426	candela/m ²	cd/cm ²	cd/cm ²	candela/m ²	0.2919	foot-lamberts	fl																
<u>FORCE and PRESSURE or STRESS</u>					<u>FORCE and PRESSURE or STRESS</u>																				
lbf	pound-force	4.45	newtons	N	N	newtons	0.225	pound-force	lbf																
psi	pound-force per square inch	6.89	kilopascals	kPa	kPa	kilopascals	0.145	pound-force per square inch	psi																
					<table style="margin: auto; border: none;"> <tr> <td style="padding: 0 10px;">-40°F</td> <td style="padding: 0 10px;">0</td> <td style="padding: 0 10px;">32</td> <td style="padding: 0 10px;">40</td> <td style="padding: 0 10px;">80</td> <td style="padding: 0 10px;">120</td> <td style="padding: 0 10px;">160</td> <td style="padding: 0 10px;">212°F</td> </tr> <tr> <td></td> <td></td> <td></td> <td></td> <td></td> <td></td> <td></td> <td>200</td> </tr> </table>					-40°F	0	32	40	80	120	160	212°F								200
-40°F	0	32	40	80	120	160	212°F																		
							200																		
					<table style="margin: auto; border: none;"> <tr> <td style="padding: 0 10px;">-40°C</td> <td style="padding: 0 10px;">-20</td> <td style="padding: 0 10px;">0</td> <td style="padding: 0 10px;">20</td> <td style="padding: 0 10px;">40</td> <td style="padding: 0 10px;">60</td> <td style="padding: 0 10px;">80</td> <td style="padding: 0 10px;">100°C</td> </tr> <tr> <td></td> <td></td> <td></td> <td></td> <td>37</td> <td></td> <td></td> <td></td> </tr> </table>					-40°C	-20	0	20	40	60	80	100°C					37			
-40°C	-20	0	20	40	60	80	100°C																		
				37																					
<p style="text-align: center;">These factors conform to the requirement of FHWA Order 5190.1A *SI is the symbol for the International System of Measurements</p>																									

ACKNOWLEDGMENTS

The authors wish to express their appreciation to the Alaska Department of Transportation and Public Facilities (Alaska DOT&PF) personnel for their support throughout this study, as well as the Center for Environmentally Sustainable Transportation in Cold Climates (CESTiCC). The authors would also like to thank all members of the Project Technical Advisory Committee. Acknowledgment is also extended to students and faculty who helped from the University of Alaska Fairbanks and Missouri University of Science and Technology.

TABLE OF CONTENTS

EXECUTIVE SUMMARY	1
CHAPTER 1.0 INTRODUCTION.....	3
1.1 Problem Statement	3
1.2 Objective	4
1.3 Research Methodology	4
1.3.1 Literature Review and Survey.....	4
1.3.2 Laboratory Testing and Optimization of Mix Design.....	4
1.3.3 Preliminary Cost Analysis and Comparison	6
1.3.4 Final Report and Recommendations	6
CHAPTER 2.0 LITERATURE REVIEW AND SURVEY.....	7
2.1 Rutting (Abrasion) Issues of PCC Pavements	7
2.1.1 General Issues/Distresses in PCC Pavements	7
2.1.2 Rutting and Durability Issues.....	7
2.2 Abrasion Resistant and Durable Concrete	10
2.2.1 Material and Design	11
2.2.2 Construction Techniques.....	17
2.2.3 State-of-the-Art Practices in Cold Climate Areas	19
2.3 Survey	24
2.3.1 Concrete Pavement Surfaces in Alaska	24
2.3.2 Potential Benefits and Drawbacks Regarding Concrete Pavements	26
2.3.3 Use of SCMs in Alaska Concrete	28

2.3.4 Discussions with Out-of-state Pavement Engineers	30
CHAPTER 3.0 SCREENING TESTS AND ANALYSIS.....	32
3.1 Materials and Specimen Preparation.....	32
3.1.1 Materials.....	32
3.1.2 Mixes.....	32
3.1.3 Mixing.....	34
3.1.4 Specimen Fabrications	35
3.2 Testing Procedures	36
3.2.1 Workability and Air Content.....	36
3.2.2 Compressive and Flexural Testing.....	36
3.3 Results.....	37
3.3.1 Workability	37
3.3.2 Air Content.....	39
3.3.3 Compressive Strength	39
3.3.4 Flexural Strength.....	42
3.4 Determining the Optimum Mix.....	43
3.4.1 Minitab Method.....	44
3.4.2 Excel Method	46
3.4.3 Results	50
CHAPTER 4.0 PERFORMANCE TESTS AND RESULTS.....	52
4.1 Materials and Specimen Preparation.....	52
4.1.1 Materials.....	52

4.1.2 Mixes.....	53
4.1.3 Mixing and Specimen Fabrications.....	54
4.2 Testing Procedures	54
4.2.1 Properties of Fresh Concrete	54
4.2.2 Mechanical Properties	56
4.2.3 Durability	56
4.3 Results	62
4.3.1 Properties of Fresh Concrete	62
4.3.2 Mechanical Properties	63
4.3.3 Durability of Hardened Concrete	65
CHAPTER 5.0 PRELIMINARY COST ANALYSIS.....	73
CHAPTER 6.0 CONCLUSIONS.....	76
CHAPTER 7.0 REFERENCES.....	80
APPENDIX.....	91

LIST OF FIGURES

2.1 Alaska DOT&PF three regions	25
2.2 Atigun River No. 2 Bridge	27
2.3 Cracks on silica fume deck at Troublesome Creek Bridge.....	29
3.1 Alaska fine aggregate gradation chart.....	33
3.2 Alaska intermediate aggregate gradation chart.....	33
3.3 Mixing and testing concrete.....	35
3.4 Preparing samples	36
3.5 Compressive and flexural strength testing.....	37
3.6 Workability of each screening mix	38
3.7 Air content of each screening mix	39
3.8 Compressive strength (ksi) vs. time (days) at 4% and 8% silica fume content	40
3.9 Compressive strength (ksi) of 8% silica fume mixes vs. time (days).....	41
3.10 Compressive strength (ksi) of 4% silica fume mixes vs. time (days).....	42
3.11 Average flexural strength of mixes and their silica fume content	43
3.12 Flexural strength (psi) of mixes with 4% silica fume content vs. time (days).....	44
3.13 Flexural strength (psi) of mixes with 8% silica fume content vs. time (days).....	44
3.14 Optimum mix as determined by Response Optimizer for Mix on Minitab	49
4.1 Missouri fine aggregate gradation chart	52
4.2 Missouri intermediate aggregate gradation chart.....	53
4.3 Sample preparation	55
4.4 Air meter	55

4.5 Measuring shrinkage.....	56
4.6 Testing abrasion by mass loss.....	57
4.7 Nordic Prall Test.....	58
4.8 Freeze-thaw testing.....	60
4.9 Preparing and testing deicing samples.....	60
4.10 Testing chloride ion penetration.....	62
4.11 Time (days) vs. length change (%).....	64
4.12 Mass loss of mixes due to abrasion testing.....	66
4.13 Prall samples after testing.....	67

LIST OF TABLES

3.1 Base mix design	34
3.2 Total cementitious material percent composition for each screening test mix.....	34
3.3 Constraints used (% cementitious material)	45
3.4 Models fit for each response	47
3.5 Response limits and importance	48
3.6 Special cubic model coefficients for each response	Error! Bookmark not defined.
3.7 Excel versus Minitab optimum mix	50
3.8 Predicted value and desirability for each response in the optimum mix	50
3.9 Mixes determined for performance testing	51
4.1 Cementitious material percent composition for the optimal and control mixes	53
4.2 Prall results interpretation	58
4.3 ASTM C672 sample degradation ratings.....	61
4.4 Chloride ion penetrability based on charge passed.....	62
4.5 Workability and air content of optimum and control mixes	Error! Bookmark not defined.
4.6 Compressive strength of optimum mixes	63
4.7 28 day shrinkage per mix	64
4.8 Prall test results	67
4.9 Visual rating at 50 days.....	68
4.10 Deicer scaling samples before and after 50 cycles	69
4.11 Durability factor of each mix	70
4.12 Chloride permeability results	71

5.1 Cost of materials in Anchorage, AK in June 2019	73
5.2 Assumed construction cost for 2-lane rigid pavement using Control SL8 Mix	75
5.3 Estimated cost of each alternative.....	75

EXECUTIVE SUMMARY

Studded tire usage in Alaska contributes to rutting damage on pavements resulting in high maintenance costs and safety issues. In this study highly-abrasion resistant concrete mix designs using supplementary cementitious materials including silica fume (SF), ground granulated blast furnace slag (SL), and type F fly ash (FA), were developed. The fresh, mechanical and durability properties of these mix designs were then tested to determine an optimum highly-abrasion resistant concrete mix, which could reduce rutting damage in cold climates. In addition to this, a survey and literature review on concrete pavement practices in Alaska and other cold climates was conducted. Lastly, a preliminary cost analysis was completed to compare each of the determined optimum mixes.

Initial screening tests on 10 mixes were completed. Tests included compressive strength, flexural strength, workability and air content. These mixes included two binary mixes containing 4% and 8% SF and eight ternary mixes of 4% or 8% SF with 23-38% SL or FA. Subsequently four optimum mixes were determined using optimum desirability functions. These mixes, along with the control 8% SF mix, were then subjected to additional performance tests. The optimal mix for workability, compressive strength and flexural strength was determined to contain 4% SF, 12% SL and 1% FA (SL12 SF4 FA1) while the optimal mix for solely compressive strength was determined to contain 8% SF, 8% SL, and 3% FA (SL8 SF8 FA3). The optimal mixes for solely flexural strength and workability were determined to 8% SF and 22% SL (SL22 SF8), and 31% FA and 4% SF (FA31 SF4), respectively.

Each mix had varied performance test results. Concerning strength and drying shrinkage at 28 days, SF8 had the highest compressive strength, while FA31 SF4 had the lowest shrinkage.

When measuring abrasion resistance using both mass and volumetric loss, FA31 SF4 had the lowest mass loss while SL12 SF4 FA1 had the lowest volumetric loss. At 50 days SL22 SF8, SL8 SF8 FA3 and FA31 SF4 all had moderate to severe scaling from deicing salts with visual ratings of four. SF8 and SL12 SF4 FA1 performed worse with severe scaling and visual ratings of five. All mixes had potentially high resistance to chloride ion ingress with all mixes but SL12 SF4 FA1 having very low ratings of 250-619 coulombs. SL12 SF4 FA1, although still having a low rating, had a 1032 coulomb charge passed. When freeze-thaw resistance was measured SF8 performed the best with a durability factor of 99% after 180 cycles while SL22 SF8 and SL12 SF4 FA1 performed the worst with durability factors of 25% and 31%, respectively. A preliminary cost analysis comparing the construction costs of each of the performance testing mixes found that the SL12 SF4 FA1 mix would have the lowest construction cost of \$1.6 million per 2-lane highway. There was minimum variance in cost though with the costs of the five mixes ranging between \$1.6 to \$1.7 million.

Given its high strength and durability in respect to freeze-thaw resistance, as well as due to the high cost of shipping large quantities of SCMs into Alaska for construction, it may be beneficial to use a binary silica fume mix for most concrete pavements. This said the ternary mixes and quaternary mixes of silica fume with either fly ash or slag, or both, could also be a good option given their desirable associated fresh, mechanical, and durability properties.

CHAPTER 1.0 INTRODUCTION

1.1 Problem Statement

Wearing course rutting that causes progressive loss of material from the surface is a typical pavement distress occurring in the Central Region of Alaska and other northern states such as Washington and Oregon (Zubeck et al., 2004). This type of pavement damage is mainly due to the use of studded tires, which are thought to improve traction on compact snow and ice, but also tend to wear away the pavement surface in the wheel path and create safety issues such as depressions (Cotter and Muench, 2010). Millions of dollars in road maintenance costs are expended to address surface course wear and deformation of our existing pavements every year (Malik, 2000; Zubeck et al., 2004). Using the best possible materials and construction practices is essential to optimizing pavement service and life cycle costs. This has led to extensive research into developing a number of experimental features deployed nationwide to evaluate various innovative concrete materials, or construction practices for concrete that may yield better performance than traditional asphalt mix, especially for pavements that are more resistant to studded tire wear.

In Alaska, concrete has been used in heavy traffic areas such as some intersections, portions of roads, and weigh-in-motion slabs on high-volume highways. Currently there are new mix design technologies proposed to reduce rutting due to studded tire wear, such as adding crumb rubber and steel fiber to concrete mixes. In the meantime, concrete with commonly used additives is already in production and appears to be more durable and cost-effective. The key is to identify the optimum concrete mix design, and produce and implement cost-effective, highly abrasion-

resistant, and durable concrete for cold region highway applications that are competitive with flexible pavement.

1.2 Objective

The objective of this research was to implement highly abrasion-resistant concrete paving through identifying and selecting concrete mix designs to provide the lowest cost at the longest service life.

1.3 Research Methodology

To meet the objective of this study, the following major tasks were completed:

- Literature review and survey
- Laboratory testing and optimization of mix design
- Preliminary cost analysis and comparison
- Final report and recommendations

1.3.1 Literature Review and Survey

A comprehensive literature search of published materials (nationally and internationally), on-going research projects on relevant materials practice and construction techniques for improving abrasion resistance, and durability of concrete pavements was completed. In addition, interviews with Alaskan materials suppliers, public works directors, contractors and Alaska Department of Transportation and Public Facilities (Alaska DOT&PF) engineers were completed. A critical analysis of the practices and information collected from these interviews was used in the development of the mix designs used in this study.

1.3.2 Laboratory Testing and Optimization of Mix Design

The key for successfully using ternary mixes is that a number of concrete mixes need to be

formulated and tested to ensure their performance; the proportions of various ingredients should be tested to demonstrate that all the required concrete properties for a specific project meet the requirements (Schlorholtz, 2004). Hence, optimizing and finalizing a concrete mix design was completed by refining existing mix designs provided to Alaska DOT&PF (the silica fume mix designs developed by Anchorage Sand & Gravel served as a reference). This was achieved by producing different mixes with varying combination and contents of SCMs (i.e. silica fume, fly ash and slag) currently used in ready-mix applications. The experimental matrix was finalized upon discussions between the research team and professionals from Alaska DOT&PF and the Alaska concrete industry. A series of lab tests for fundamental engineering properties and durability performance of concrete were conducted, including:

- Workability (slump test for fresh concrete mixes, ASTM C143)
- Air content (AASHTO TP118 for Super Air Meter and ASTM C231 for Standard Air Meter)
- Mechanical properties related tests
 - compressive strength (ASTM C39)
 - flexural strength (ASTM C78)
 - shrinkage potential (ASTM C157)
- Durability tests
 - wear resistance (ASTM C944 and ATM 420 Abrasion of HMA by the Prall Test, Method A)
 - freeze-thaw cycling resistance (ASTM C666)
 - resistivity – concrete’s ability to resist chloride ion penetration (ASTM C1202)
 - frost scaling resistance after freezing-thawing cycle (ASTM C672)

All mechanical properties were tested at 7, 14, and 28 days. In addition, as a basic performance indicator, compressive strength was tested at 1 and 3 days to capture the early age characteristics of the material and to compare results at standard test ages, such as the 28 day test age. The effects of design parameters on mechanical properties were investigated to narrow the selection of parameters and determine the optimum mix designs.

Durability testing was conducted at 28 days except freeze-thaw cycling resistance which was tested at 14 days as per ASTM C666. The air content of the screening test mixes was measured using a Super Air Meter following AASHTO TP118. The air content of the performance test mixes was measuring using an Air Meter following ASTM C231.

1.3.3 Preliminary Cost Analysis and Comparison

A preliminary cost analysis was conducted to estimate the cost differentials of the optimum designs determined.

1.3.4 Final Report and Recommendations

A final report was completed upon the completion of previous tasks. The report included a summary of literature review and survey responses, descriptions of procedures and results from the laboratory testing, the optimization process for determining the optimum mix designs and a preliminary cost analysis comparing the concrete pavement options. The project's findings were also outlined and future areas of research were recommended.

CHAPTER 2.0 LITERATURE REVIEW AND SURVEY

In this chapter, a comprehensive literature review was performed on published materials regarding some common distresses; particularly the rutting and durability issues associated with the Portland Cement Concrete (PCC) pavements and current practices in producing abrasion-resistant PCC pavements. Further review was also dedicated to the material, design, and associated construction techniques required by abrasion-resistant cement concrete pavements. In addition, state-of-the-art practices regarding abrasion-resistant cement concrete pavements in cold region states were reviewed.

2.1 Rutting (Abrasion) Issues of PCC Pavements

2.1.1 General Issues/Distresses in PCC Pavements

PCC may deteriorate due to inadequate design and construction practices, lack of maintenance, or inadequate specified concrete. As summarized in Hobbs (2001), deterioration in structural concrete members is mainly due to the corrosion of reinforcing steel induced by chloride ion ingress into concrete, freeze-thaw cycle, abrasion, carbonation induced corrosion, alkali-silica reaction (ASR), and external and internal chemical attack. The deterioration of cement concrete could result in distresses such as scaling, cracking (i.e. durability cracking, longitudinal cracking, and transverse cracking), polished aggregate, rutting, and water bleeding and pumping (Miller and Bellinger, 2003; Won et al., 2002). In cold region states, the distresses of rutting and the associated loss in durability deserves special attention due to the use of studded tires.

2.1.2 Rutting and Durability Issues

In cold regions, studded tires are typically used to increase traction during icy conditions, which can also improve safety and allow increased speeds. The relationship between studded tires and

pavement wear is well-established (Angerinos et al., 1999; Malik, 2000; Zubeck et al., 2004). As suggested by Lundy et al. (1992), contributions of wear from studded tire abrasion in pavement rut development must not be ignored when factors in pavement rutting are analyzed. Not only does studded tire usage contribute to pavement wear and rutting, but rutting is also caused by the plastic deformation of the pavement due to heavy vehicles (Zubeck et al., 2004). However, studded tires cause the majority of rutting in areas where studded tires are used. As summarized by Cotter and Muench (2010), studs are likely responsible for nearly 100% of wheel path wear on Washington PCC pavement. Niemi (1978) identified four mechanisms that contribute to pavement wear:

- 1) The scraping action of the stud produces marks of wear on the mastic formed by the binder and the fine-grained aggregate.
- 2) The aggregate works loose from the pavement surface because of scraping by studs.
- 3) Scraping by the stud produces marks of wear on stones, but only in very soft aggregate does a rock fragment wear away completely by this action.
- 4) A stone is smashed by the impact of a stud and the pieces are loosened by the scraping action of the stud.

Rutting can be an issue for cement concrete pavements in cold regions due to the use of studded tires in winter time (e.g. Anderson et al. 2007, Anderson et al. 2009; Cotter and Muench 2010; Anderson et al. 2011). Studded tires are known to cause accelerated wheel path wear resulting in additional pavement preservation costs. Anderson et al. (2007) stated that wear on PCC pavement and the associated rutting issue was primarily due to the use of studded tires. Outside of studded tires, several other factors which can influence the rate of pavement wear have been

identified as summarized in Keyser (1971). These influencing factors generally include the vehicle (i.e. axle load, tire number, and stud type), pavement (i.e. geometry, surface material, and surface condition), environment (i.e. moisture and temperature), and traffic (i.e. volume, speed, wheel track, and contact mode). As stated in the Washington State Department of Transportation (WSDOT) 2006 report, studded tires were prohibited in Washington State until 1969. Data collected from Washington highways indicated that roadway surface wear was increasing at a considerable rate in three winter seasons after studded tires were allowed. This result persuaded the legislature to restrict the use of studded tires to the period from November 1st to March 31st. Since then Washington has continued to introduce legislation to limit and discourage the use of studded tires in an attempt to reduce pavement wear on the highway system. According to Cotter and Muench (2010), the average PCC pavement in Washington State wears at about 0.01 inches per one million studded tire passes. They found the highest wear rates were near 0.02 in./year on I-90 in the Spokane area, while the lowest wear rates were in the range of 0.002 -0.004 in./year in other locations. It was also found that the stud wear rates were generally higher in the first five years of PCC pavement life and much less thereafter. Malik (2000) investigated pavement wear and the costs of mitigating studded tire damage in Oregon. A wide range of wear rates were found for various sections of PCC and asphalt pavements. PCC was found to be more resistant to rutting with an average wear rate on PCC pavements of 0.01 in. per 100,000 studded tire passes. In comparison, the asphalt pavements studied had over four times this wear rate with a rate of 0.04 in. per 100,000 studded tire passes. Further evaluation conducted by Shippen et al. (2014) had similar findings with wear rates of 0.231 mm and 0.749 mm per 100,000 studded tire passes for PCC and asphalt pavements, respectively.

The rutting issue due to the use of studded tires inevitably leads to a reduction in the durability of PCC pavements. The costs for repairing these pavements also rise through accelerated pavement wear due to studded tire use. As a result, highway agencies, including the Federal Highway Administration (FHWA) supported efforts to ban or limit the use of studded tires to lower the yearly pavement rehabilitation costs attributed to studded tire usage. A 1974 Oregon Department of Transportation (ODOT) report estimated that if the studded tire winter usage rates continued at 9.2% the associated pavement wear would result in 90 lane miles needing to be resurfaced each year with an annual cost exceeding one million dollars (ODOT, 1974). A more recent 2016 estimate for WSDOT showed that studded tire usage could result in a \$12 to \$18 million annual damages to PCC pavements, which represent only 13% of the state road network (WSDOT, 2016). An older report also estimated that approximately 234 miles of PCC pavement lane in Washington State exceeded the threshold for repair based on rut depth criteria (> 10 mm) (WSDOT, 2006). Because of this, the use of studded tires in the summer is prohibited in most states. Outside of the U.S., Finland, Sweden and Norway have also conducted a substantial amount of research on studded tire issues and have successfully reduced their wear rates through wear resistant pavements, less aggressive studs and strictly enforced seasonal studded tire usage (Zubeck et al., 2004).

2.2 Abrasion Resistant and Durable Concrete

A great deal of research effort has been dedicated to increasing the durability of PCC pavements through use of supplementary cementitious materials (SCMs). The most recent research on SCMs has focused on a few areas: exploring new materials, increasing replacement amounts, developing better test methods, treating or modifying materials, and using additives to improve

performance of the PCC. A review on the existing SCMs and the associated design and construction techniques are presented in the following sections.

2.2.1 Material and Design

2.2.1.1 SCMs

SCMs are commonly used as a replacement for a portion of the clinker component in cement, or as a replacement for a portion of the cement component in concrete (Juenger and Siddique, 2015). Typical SCMs include fly ash, silica fume, and slag, as well as other materials continuously entering the market such as natural pozzolans and alternative SCMs (Sutter, 2016). Fly ash mainly consists of SiO_2 , significant quantities of Al_2O_3 , and variable amounts of CaO , depending on the material origin (Lothenbach et al., 2011). Fly ash is the most common SCM used in concrete, with the first results recorded in the 1930s (Davis et al., 1937). Blending cement with fly ash has numerous benefits including: increased late strength, decreased shrinkage and permeability, improved workability, decreased heat of hydration, potential increased sulfate resistance and ASR mitigation, and reduced concrete costs (Schlorholtz, 2004). In Atiş (2002) fly ash was used to replace the cement in mass basis at 50 and 70% in concrete mixes with various water to cementitious material (w/c) ratios. Test results showed that for high strength grades (>40 MPa), the abrasion resistance of the 70% fly ash concrete was higher than both that of the ordinary Portland cement (OPC) concrete and the 50% fly ash concrete. Obla et al. (2003) discussed the fresh and hardened properties of concrete made with an ultra-fine fly ash (UFFA) produced by air classification. Durability tests were also conducted to determine the chloride diffusivity, rapid chloride permeability, ASR, and sulfate attack. Test results indicated that at a given workability and water content, concrete containing UFFA could be produced with

only 50% of the high-range water-reducer (HRWR) dosage required for comparable silica fume concrete. Similar early strengths and durability measures as the silica fume concrete were also observed when a slightly higher dosage of UFFA was used with a small reduction in water content.

Slag, or slag cement, has been used in Portland cement since 1896 (ACI, 2011). Blast-furnace slag contains more CaO but significantly less Al_2O_3 than fly ash (Lothenbach et al., 2011). Blast-furnace slag is granulated to produce hydraulic slag cement that produces calcium silicate hydrate as a hydration product similar to OPC. The reaction of slag cement with water is slower than that of OPC, thus developing strength over a longer period and leading to reduced permeability and better durability (Sutter, 2016). Osborne (1999) investigated the performance and long-term durability of concrete where ground glassy blast-furnace slag (granulated and pelletized) has been used as a cementitious material. When adding slag to concrete, several technical benefits were identified such as reduced heat evolution, lower permeability and higher strength at later ages, decreased chloride ion penetration, and increased resistance to sulfate attack and ASR. In addition, guidance was provided for the design, specification, application and performance of concrete in practice where slag can be used to reduce costs and energy demands in the production of cement compared with normal Portland cement.

Silica fume consists nearly exclusively of very fine and amorphous SiO_2 which is highly pozzolanic (Lothenbach et al., 2011). Mainly due to the pozzolanic reactions as well as its particle size (Detwiler and Mehta, 1989), silica fume has been found to significantly improve the abrasion resistance of concrete (Ghafoori and Diawara, 1999), mitigate the potential for sulfate attack, alkali-aggregate reactions, and corrosion of reinforcing steel in concrete (Justnes, 2007).

A high-strength silica fume concrete was used to rehabilitate two structures which had suffered severe abrasion-erosion damage, and the repairs showed adequate abrasion resistance with a mix containing 15% silica fume by mass of cement (Van Dam, 2014). Increasing silica fume content up to 15% continuously has been found to improve the abrasion resistance of self-compacting concrete (Turk and Karatas, 2011). The fine particle size also demands increased water, leading to the use of HRWRs to maintain or decrease the w/c ratio of the mix (Sutter, 2016).

The concept of adding two SCMs in the binder fraction of OPC to produce ternary concrete mixes can be traced back nearly 60 years ago (Abdun-Nur, 1961). This process is becoming more prevalent because the benefits of using ternary mixes, such as enhanced performance and cost reduction, are gradually becoming apparent (Schlorholtz, 2004). Generally, ternary mixes show overall better performance as negative properties of any one SCM can be offset by positive properties of another carefully selected material (Sutter, 2016). For example, blending an ultrafine pozzolan, such as silica fume, with slag or fly ash can prevent excessive bleeding problems by offsetting the increased water demand typically associated with the use of silica fume (Bleszynski et al., 2002; Thomas et al., 1999). Higher 28-day compressive strength was reported when comparing a ternary mix containing 20-25% slag and 3-5% silica fume to a control mix (Thomas et al., 2007). Many improved durability characteristics have been reported on ternary mixes when proportioned accurately, including better chloride resistance (Wongkeo et al., 2014), higher resistance to ASR (Shehata and Thomas, 2002), better scaling resistance (Radlinski et al., 2008), and less deterioration after freeze-thaw cycles (Rupnow, 2012).

An increase in abrasion resistance is also an important benefit provided by ternary concrete mixes. Scholz and Keshari (2010) found that, when compared with the control mix, a mix with

4% silica fume and slag demonstrated significantly higher abrasion resistance, but increasing silica fume beyond 4% did not add further benefits. Rashad et al.'s (2014) study indicated that high-volume fly ash (HVFA) concrete blended with either silica fume or equal combinations of silica fume and granulated blast-furnace slag (GGBS) showed higher abrasion resistance, while lower abrasion resistance was found in HVFA blended with GGBS. Another study of ternary concrete mixes with different proportions of low calcium class F fly ash (20%, 30%, or 40%) and silica fume (5% or 10%) found the ternary mix containing fly ash up to 30% and 5% silica fume showed better performance against abrasion erosion (Ramana et al., 2014). Yener and Hınısliođlu (2011) investigated the effects of silica fume and fly ash additives on the frost salt scaling resistance, durability, and flexural strength properties of pavement concrete. Silica fume and fly ash were used as cement replacement in proportions of 0, 5, 10%, and 0, 5, 10, 15% by weight, respectively. Experimental results indicate that using silica fume and fly ash together resulted in increased strength and better scaling resistance than the control mix (i.e., OPC). Hamilton et al. (2009) evaluated the durability of concrete made with a ternary blend of cementitious materials that included ordinary Portland cement, fly ash, and blast furnace slag in comparison to the current practice of using silica fume. Test results showed the mixes with higher fly ash (30 to 40% by replacement weight) content had delayed gains in compressive strength. Increasing quantities of slag (and associated decrease of Portland cement) produced a slight decrease (<10%) in average seven day compressive strength. Also, the mixes containing both fly ash and slag were improved compared to that of the control binary fly ash mix. Hossain et al. (2009) evaluated the influence of the combination of UFFA and silica fume on the properties of fresh and hardened concrete. They also compared the performance of concrete

incorporating UFFA and silica fume (a ternary blend of cement), concrete incorporating ultrafine fly ash or silica fume (binary blend of cement), and control PCC. The test results found that the incorporation of UFFA or silica fume in concrete resulted in higher strength and improved durability (resistance to chloride penetration). These benefits were more pronounced in the silica fume concrete. However, the silica fume concrete demonstrated several limitations such as low slump and high early-age shrinkage, while the addition of UFFA resulted in increased slump and lower early-age shrinkage. To minimize the shortcomings of silica fume without losing its strength and durability benefits, a ternary mix of both UFFA and silica fume was tested. Results found that the incorporation of both silica fume and UFFA produced a concrete mix that demonstrated high early-age strength and improved durability similar to those properties in silica fume concrete. In addition, unlike a binary silica fume concrete, the new concrete mix demonstrated a higher level of slump and a lower level of free shrinkage.

2.2.1.2 Other Innovations

Li et al. (2006) experimentally investigated the abrasion resistance of concrete containing nanoparticles (i.e. nano-TiO₂ and nano-SiO₂ with an average particle size of 10-15 nm, which is much smaller than the size of the UFFA), plain concrete, and concrete containing polypropylene fibers. Test results indicated that samples containing nano-TiO₂ particles had the highest abrasion resistance, followed by those containing nano-SiO₂ particles, polypropylene fibers, and lastly the control mix. The abrasion resistance of concrete containing nanoparticles was also found to linearly increase with increasing compressive strength.

Recently, different types of fibers such as asbestos, cellulose, steel, polypropylene, basalt, and glass have been used to modify cement products as summarized in Hannant (2003). The

introduction of fibers in concrete can also improve concrete durability. In Kabay (2014), basalt fiber was introduced to both high strength and normal strength concretes which were cast with different water-to-cement ratios. An improved abrasion resistance was obtained by using basalt fiber even at low contents. A strong relationship was also established between abrasive wear and both the void content and flexural strength of the concretes. However, the inclusion of basalt fiber in concrete resulted in a reduction in the compressive strength. As presented in Grdic et al. (2012), two types of polypropylene fibers were added to both classic and micro-reinforced concrete to improve the abrasive resistance of the concrete. The w/c ratio varied from 0.5 to 0.7, while the content of the remaining components was held constant. An accelerated test was performed, which allowed the high-velocity jet of water/sand mix to act on the surface of the test specimens, to determine the abrasive erosion of concrete. Test results indicated that the addition of polypropylene fibers has a positive effect and contributes to increased resistance to abrasive erosion. Thus, for the w/c ratio of 0.5, the addition of monofilament polypropylene fibers of FIBRILs S120 and F120 types improved the abrasive resistance of concrete by 7.08% and 13.47%, respectively. Similar increases in abrasive resistance were also determined for the w/c ratios 0.6 and 0.7. The micro-reinforced concretes demonstrated higher abrasive resistance in comparison to the control concrete. In addition, the abrasion resistance was found to be in an inverse function of the water-to-cement ratio; concretes with higher compressive strength and higher bending strength also had higher abrasive resistance.

In recent years, resin has been used in conjunction with hot mix asphalt (HMA) to resist rutting and abrasive traffic primarily on military bases. Resin modified pavement is a surface overlay of an open-graded HMA mix where 25-35% of air voids are filled with a latex-rubber modified

Portland cement grout. In the overlay procedure, the open-graded mix and grout are produced and placed separately, resulting in a 1.8 to 2.5 in. thick composite material. The additive was believed to increase the flexural and compressive strength of the hardened material, thus increasing abrasion resistance, and potentially studded tire wear as well (Battey and Whittington, 2007). For the most part resin-modified pavement is used as a rehabilitation overlay; however, it can also be used with new construction as well. Often it is placed over a pavement that has already been rehabilitated with HMA (AFCESA/CES, 2001).

In Mississippi resin modified pavement test sections were placed on two HMA pavement intersections on US 72 with histories of traditional rutting (from pavement deformation) (Battey and Whittington, 2007). After five years of observation, the Mississippi DOT published a final report in 2007 that featured both positive and negative reviews of their experience with resin-modified pavement. In this final report, the performance measurements also showed skid resistance below state standards. The major positive result of the project however was that after five years there was no rutting (Mississippi does not allow studded tires so this was a measure of plastic flow deformation rutting and not stud wear) reported on the resin modified pavement sections and overall pavement condition ratings were acceptable. The resulting pavement appears to be successful in its goal of withstanding abrasive traffic, heavy static loads, and channelized traffic, however the construction practices have not been perfected, and long term observation is needed (Battey and Whittington, 2007).

2.2.2 Construction Techniques

As discussed above, different SCMs, nano-particles, and polypropylene fibers have been used as additives to modify PCC. However, the construction techniques for these additives are different.

Obla et al. (2003), when adding UFFA to concrete, prepared the concrete according to ASTM C192 except they extended the mixing time by two minutes. Later the high-range water reducer was added after the concrete achieved a plastic state with 13 mm (0.5 in.) slump. When silica fume is added to the concrete, there was some concern over properly dispersing the agglomerated silica fume particles. Previous studies had shown that densified silica fume particles are not always broken up adequately during standard lab mixing procedures according to Fidjestel et al. (1989). The Silica Fume Association created a special silica fume user's manual that contained a recommended proportioning procedure (see: <http://www.silicafume.org/pdf/concrete-labmix.pdf>). Based on this manual, as presented in Van Dam (2014), 75% of water was placed in the mixer along with the coarse aggregate and silica fume. This was mixed for 90 seconds and then the remaining cementitious materials were added and mixed for an additional 90 seconds. Following this the remaining water and fine aggregate was added to the mixer and mixed for five minutes. Following a three-minute rest period, the mix was mixed for a final five minutes. The total time of 16 minutes for this procedure was significantly longer than eight minutes outlined in ASTM C192.

In Li et al. (2006), to fabricate the concrete containing nano-particles, first a water reducing agent and the water was mixed in a mortar mixer. Then nano-particles were added and stirred at high speed for five minutes. The defoamer was added during stirring. Cement, sand and coarse aggregate were mixed at a low speed for two minutes in a concrete centrifugal blender, and then the mix of water, water-reducing agent, nano-particles and defoamer was slowly poured in and stirred at a low speed for another two minutes to achieve good workability. To fabricate both the plain concrete and the concrete containing polypropylene fibers, a water-reducing agent was first

dissolved in water. Then the cement, sand, coarse aggregate and polypropylene fibers were mixed in a concrete centrifugal blender. The mix of water and a water-reducing agent was then poured in and stirred for several minutes. After pouring, an external vibrator was used for compaction and to decrease the number of air bubbles. Finally, the fresh concrete was obtained.

2.2.3 State-of-the-Art Practices in Cold Climate Areas

In some cold climate areas, current state-of-the-art in material technology and pavement design has allowed for implementation of improved materials and pavement sections that are resistant to rutting. WSDOT has conducted a series of experimental feature studies to address the tire wear resistance of PCC pavements (Masad and James 2001; Anderson et al. 2007, 2009, 2011; Cotter and Muench 2010). Anderson et al. (2009) investigated the effects of traffic and stud wear for WSDOT on combined gradation concrete by comparing the rutting on standard near gap graded PCC with a uniform combined gradation PCC. Two sections of pavement were built with different specifications for the gradation of the aggregates, one with the standard WSDOT specification and the other with a combined gradation, to determine if the use of the combined gradation would result in a pavement more resistant to studded tire wear. The standard gradation can result in a gap-graded aggregate whereas the combined gradation produces a more uniform gradation. WSDOT monitored the wear on both pavements and made analytical adjustments based on traffic volumes and the two-year age difference of the pavements. The combined gradation mix produced a higher average compressive strength with less deviation and less failed specimens than the standard mix, however, the wear rates on both road sections were approximately the same as reported in Anderson et al. (2007).

In Anderson et al. (2011), research efforts included the use of combined aggregate gradations,

ultra-thin and thin white topping, experimental finishing methods such as longitudinal tining and carpet drag texturing, higher flexural strength mix designs, high cement content mix designs, and special additives. Test sections established in 2004 and 2005 (Anderson et al., 2009) included both carpet drag and tined finish for standard 650 psi flexural strength mixes and mixes with a higher 800 psi flexural strength. The sections built in 2005 were found to have much higher wear rates than those built in 2004. The data indicated that there was an initial high rate of wear when the pavement was first exposed to studded tires and then a stabilization of the rate with time. This could be attributed to the paste on the surface of new concrete wearing off, for once the paste was gone the aggregate would wear at a much slower rate. Additionally, two sections were also developed with tined finishes, one with 650 psi flexural strength mix and Hard-Cem concrete hardener, and the other with a high cement content design similar to an SHRP SPS-2 900 psi flexural strength mix. The cement used in all the sections contained 20-25% slag. The 650 psi flexural strength mix with tined finish was produced as a control section.

The roadway paving section used consisted of one foot of doweled PCC pavement over either the existing surfacing, which was rototilled, or over areas where the existing pavement was completely removed. The PCC pavement was placed over a 0.2 foot asphalt concrete pavement over a 0.25 foot crushed surfacing base course. The paving operation began with the dump trucks unloading the wet concrete in front of the paving machine and ended with joint sawing after the application of the astro turf carpet drag finish. Two paving machines were used for the lanes poured in 2004. The first machine, a two-track paver, was used to spread the concrete in front of the second paver. The second paver, which was a four track paver, consolidated the concrete and inserted the dowel bars. The first paver would then spread the concrete so there would be a

consistent amount of concrete in front of the second paver. The westbound lanes placed in 2005 were paved using only the four track paver. An analysis of the profilograph traces did not reveal any substantial differences in ride between the two paver and single paver operations.

The contractor described the details concerning the special carpet drag finish as noted in the following excerpt from the contract as presented in Anderson et al. (2009): “The pavement shall be given a final finish surface by drawing a carpet drag longitudinally along the pavement before the concrete has taken an initial set. The carpet drag shall be a single piece of carpet of sufficient length to span the full width of the pavement being placed and adjustable to have up to four feet longitudinal length in contact with the concrete being finished. The carpeting shall be artificial grass type having a molded polyethylene pile face with a blade length of 5/8 -1 inch and a minimum mass of 70 ounces per square yard. The backing shall be a strong durable material not subject to rot and shall be adequately bonded to the facing to withstand use as specified.”

Early wear measurements were conducted in 2006. The results did not point to any mix design outperforming any other, although the amounts of wear and the highest wear rates were held by the sections that were built with the tined finish. The average friction numbers for all sections were tightly grouped between 30.2 and 41.6 with the highest averages belonging to the sections with tined finishes. In general the ride measurements decreased slightly with age for all sections with the greatest decreases noted for the youngest sections paved in 2005 (Anderson et al. 2009). Anderson et al. (2011) summarized wear, ride and friction measurements made every spring and fall from 2006 to 2010. This research showed that using a mix with higher flexural strength, higher cement content, or the additive Hard-Cem did not result in a concrete mix that was more resistant to studded tire wear than the WSDOT conventional 650 psi flexural strength mix

design. In addition, no correlation was found between the amount of wear and the experimental features evaluated in the study (i.e., the method used to finish the concrete, measured flexural strength and the design). The study found that the mix design with a standard 650 psi flexural strength showed equal or better resistance to studded tire wear over that of any of the other mix designs examined. However, it should be noted that slag was the only SCM used in this study. Other potential SCMs, such as fly ash and silica fume or ternary concrete mixes determined to provide superior abrasion resistance, were not considered.

As summarized in Cotter and Muench (2010), excessive stud wear problems were limited and not a widespread issue in Washington State. Most pavement sections showed reasonably small wear rates. It is likely that a project-specific factor rather than general wear issues drive excessive wear rates. The most plausible explanation was that some projects have knowingly or unknowingly used a softer aggregate. Regarding PCC pavement rehabilitation, diamond grinding was the most cost-effective measure, especially to correct stud wear in Washington. HMA overlays were also a viable option, although they were just as susceptible to stud wear as PCC and thus were likely to suffer a recurrence of the same stud wear problem.

There are alternatives to the current design for studded tires that offer some improved winter traction on compacted snow and ice. These include all-season tires, retractable studs, and lighter-weight studs, GoClaw, and Green Diamond Tires, as summarized in Cotter and Muench (2010). Alternatively, concentration can instead focus on anti-icing measures to improve winter traction rather than tire technology. Currently there are no tests to accurately predict studded tire wear on PCC pavement. There are three main tests that are sometimes used to estimate wear: Nordic Ball Mill, Los Angeles Abrasion, and Micro-Deval. Among research on these tests there is significant

conflicting evidence as to the accuracy and ability to predict stud wear (Cotter and Muench, 2010). The Micro-Deval test has so far been the most favorably rated test, but it too has its detractors. To account for future thickness loss associated with diamond grinding, WSDOT current practice of designing an extra inch of pavement is a sound policy. In general, the use of harder aggregate seems to slow studded tire wear. Therefore some agencies use the hardest aggregate available (as measured by durability and abrasion tests) for roadways with high wear potential. Alaska has done a fair amount of work to reserve the use of premium hard aggregate for roadways with volumes susceptible to stud wear (Kuennen, 2004). Although this work has mostly focused on HMA, the results are also relevant to PCC stud wear prevention.

Badr (2010) carried out an experimental study to investigate the effect of silica fume on the freeze-thaw resistance of concretes subjected to slow freeze-thaw cycles. Concrete specimens were exposed to slow freeze-thaw cycles after seven and 28 days of initial curing. The deterioration and residual strength of concrete specimens were assessed after 25, 50 and 100 cycles. The results showed that the residual strength of mixes containing silica fume were significantly higher than those of PCC. In addition, specimens with silica fume showed less deterioration compared to specimens without silica fume. Janotka (2007) reported the behavior of concrete containing silica fume and superplasticizer Melment subjected to temperatures up to 200°C followed by 100 freeze-thaw cycles in regime of 8 hours in water at 20°C and 16 hours at -20°C. It was found that the strength, elastic modulus and volume deformation of concrete was irreversibly influenced by either the temperature elevation or rapid cooling to 20°C. When comparing the strength, elastic modulus, and shrinkage or expansion of samples exposed to 100 freezing and thawing cycles, to samples kept in water, the difference was negligible.

2.3 Survey

Alaska DOT&PF material engineers and lab technicians, a bridge engineer, researchers, private contractors, concrete suppliers, and public work directors in Alaska were surveyed about their experience regarding concrete pavements in Alaska and efforts made to combat abrasion resistance in concrete pavements. Because there are few concrete pavements in Alaska, to gain perspective from a state that regularly installs concrete pavements, two Wisconsin Department of Transportation (WisDOT) pavement engineers were also surveyed.

2.3.1 Concrete Pavement Surfaces in Alaska

There are only a few concrete pavements in Alaska. In Alaska's central region (Figure 2.1), there are some concrete intersections in Anchorage including the high-traffic intersections at 5th street and E street, and 6th street and F street (Johnson, 2019), as well as some low traffic intersections located in residential areas (Schlee, 2019). The Anchorage International Airport, at one point had concrete pavement, but is being repaved with asphalt. Nonetheless there are some concrete hardstands at the Anchorage airport where planes park (San Angelo, 2019). In the northern region of Alaska the only places where concrete and vehicle tire wheels intersect is on bridge decks and some weigh in motion slabs (Currey, 2018). There are some concrete pavements at both the Fairbanks International Airport, where there are concrete hardstands where planes park (san Angelo, 2019), and the Ft. Wainwright Airport (Mappa, Inc. 2018). The Eielson Airport was also concrete but has since been paved over with asphalt (Connor, 2019).

In Southcoast Alaska there are concrete pavements in communities including Petersburg, Wrangell and Ketchikan (Harai, 2019; san Angelo, 2019). Ketchikan had concrete roads as early as the 1960s (Connor, 2019). Although some still remain, many have been paved over with

asphalt concrete (Hilson, 2019). Howell indicated that there are around a half dozen streets paved with concrete with all but one, their main street, around 20 years old. The only concrete road Wrangell has redone is their main street, which was redone in 2011 after 37 years and now contains fiberglass fibers. Magnesium chloride deicers are applied each winter to these pavements with limited to no durability issues reported (Howell, 2019).



Figure 2.1 Alaska DOT&PF three regions (Alaska DOT&PF website)

One concrete wearing surface many respondents mentioned is the 1600 foot long main street in Petersburg. The public works director at the time of construction, Hagerman (2019), cited longevity and cost as the reason concrete was chosen. Asphalt is expensive in Petersburg because there is no local HMA plant. In addition, when the concrete pavement needs to be patched, concrete can be drawn from a local concrete plant. The main street of Petersburg has been paved with concrete since the 1960s, which was first replaced in 1985 and later in 2012. The 2012 design consisted of a six inch class A-A concrete with a two day required compressive strength of 2500 psi and a 1½ pounds per cubic yard dosage of synthetic fiber reinforcement. A class A-A concrete is considered as a “concrete where improved strength and durability is required”

(Alaska DOT&PF, 2017). Sand was provided the first winter to mitigate use of deicers, but deicers have been used since with no major deterioration (Hagerman, 2019).

Although they are not highway pavements, there are eight weigh-in-motion (WIM) slabs located throughout Alaska near Anchorage, Fairbanks, Tok, and Soldotna, of which many have a concrete surface. Gartin and Saboundjian (2005) measured the rut depth of two PCC WIM slabs in Anchorage and compared their rutting to nearby asphalt pavements of the same age and experiencing the same traffic. The PCC surfaces of WIM sites at Tudor Road and Minnesota Road had 29% and 38% less rut depth, respectively. Data on the mix design of the WIMs studied was unavailable, but a 2010 mix design of the WIM slab near Tok found it to be a class A 6.5-sack 4500 psi mix design with a 0.36 water-to-cement ratio (Mack, 2010). Rutting rates also vary by region, with minimal reported rutting problems in Alaska's northern region (Currey, 2018). Most concrete bridges in Alaska are paved over with asphalt after construction to protect the concrete (Marx, 2019). There are some bare concrete bridge decks including those on the Dalton Highway and in some low-traffic rural areas (Marx, 2019). An example of a bare concrete deck would be the Atigun River No. 2 Bridge on the Dalton Highway that was built in 2000. Almost 20 years later and the time marks are still visible (Figure 2.2). Many of the bridges built during the 1940s also have bare concrete decks. Typically bridges are usually overlaid with asphalt for protection so once the asphalt layer is damaged, the decks can easily be repaired (Marx, 2019).

2.3.2 Potential Benefits and Drawbacks Regarding Concrete Pavements

When queried about the use of concrete pavements in Alaska, many respondents voiced concerns. For example, concrete pavements generally have a higher initial cost and require a thicker pavement layer over that of asphalt pavement, and there were concerns over having to

pay for a high quality pavement just for it to fail. Some mentioned there is likely not enough traffic to make it cost-effective for most of Alaska. Others noted that concrete pavements might have similar or worse rutting resistance than asphalt. Some mentioned the potential for frost heave and thaw settlement when using concrete pavements. Regarding construction, the challenge of quality control when placing in rural locations, or having to shut down traffic in urban areas for long periods of time were also listed as concerns since concrete takes a long time to set up and cure (Brunette, 2019) and some construction sites may not have alternative routes. Another person noted that a skilled crew is required to place a concrete pavement, and some contractors do not have experience working with it on a large scale, such as for highways. Since Alaska is an oil-producing state, and needs to import cement, using asphalt is a good way to use local resources. Maintenance concerns that rigid pavements can be challenging and expensive to repair were also listed. Regarding driving on it, the noise and smoothness of driving on rigid concrete was also a concern. Lastly, when using rigid pavements on bridge decks, the rigid pavements are heavy, which affects load ratings, and may crack.



Figure 2.2 Atigun River No. 2 Bridge (Alaska DOT&PF Bridge Section, 2018)

Some benefits were also voiced. For example, most rural communities do not have an asphalt plant, but many have local concrete plants which are used for small projects, such as foundations.

Therefore, for smaller projects and for patching it could be cost-effective to use concrete instead of bringing in an asphalt plant. Some southeast communities, such as Skagway, already do this and do road patchwork on asphalt roads with concrete. Dave Johnson with Anchorage Sand and Gravel (2019) noted that despite the common belief that construction workers need to wait 28 days before opening a section to traffic, “you can do it in a weekend.” Johnson and Schlee also noted that although there are concerns over access to utilities located underneath roadways, design considerations can be made to accommodate this, as shown by cities such as Chicago and Minneapolis, which have concrete intersections. Another location concrete pavements could be used would be at roundabouts where flexible pavements have a tendency to push and shove and get ripples in hot weather (San Angelo, 2019).

2.3.3 Use of SCMs in Alaska Concrete

Most concrete mixes in Alaska do not use silica fume, slag, or fly ash. However, there have been some instances when silica fume was used. Historically a silica fume concrete mix was used on bridges decks in Alaska, but this practice has been abandoned because it was expensive, heavy, and tended to crack (Figure 2.3). Within the last decade, this practice has been phased out and replaced by polyester synthetic concretes, which do not shrink or crack (Marx, 2019). Other projects that used silica fume in their mixes include the downtown Anchorage intersections, which were paved in the late 2000s with 7-sack 5% silica fume mixes (Johnson, 2019). One benefit to using silica fume over slag or fly ash would be that a 4-8% silica fume content can improve the concrete’s properties, but higher contents (which incur higher shipping costs) are needed when using slag or fly ash (Schlee, 2019).



Figure 2.3 Cracks on silica fume deck at Troublesome Creek Bridge (Alaska DOT&PF Bridge Section, 2018)

Outside of airports and some military sites, where blended fly ash mixes are used to adhere to either USACE or FAA requirements for ASR mitigation (Schlee, 2019; Schaefer, 2019), no one could recall a concrete pavement containing fly ash in Alaska. This may be because the cost of fly ash is roughly double that of cement and the benefits of its use do not typically outweigh the cost. If a project did require fly ash, it would need to be imported with a high shipping cost.

There is one operating surface coal mine, the Usibelli Coal mine, in Alaska, which supplies six coal plants ("Statewide Socioeconomic Impacts of Usibelli Coal Mine, Inc.", 2015).

Unfortunately the fly ash produced at these plants can't be used in PCC due to its high unburnt carbon content (Sonafrank, 2010). Marx (2019) noted there might be one coal-burning facility that could produce fly ash clean enough to be used in concrete, but using this ash is likely not feasible. Although fly ash could be reburnt for use in PCC, doing so is likely not economical given the limited amount of cement used in Alaska.

Similar challenges were cited when asked if ground granulated blast furnace slag (GGBFS) was used. Because of shipping costs, slag is usually not used even if it is free (San Angelo, 2019).

Schlee did note that slag typically cost less than fly ash, but was still much more expensive than cement. For both fly ash and slag, he said that when it was used, it was to mitigate ASR, not to improve durability. The only reported location of a slag cement being used was at Ft.

Wainwright, which is located near Fairbanks. These 5.5-sack mixes, used for airport paving, had a 0.40 w/c ratio and a 40% slag content. A recent 2018 visual inspection on four of these, aged 2-10 years, found no durability issues related to freeze-thaw cycles (Mappa Inc., 2018).

2.3.4 Discussions with Out-of-state Pavement Engineers

Alaska is one of eight states that have no reported concrete arterial or collector roads (FHWA, 2018). Therefore to better understand other state DOT's experiences with concrete pavements, pavement engineers at WisDOT were surveyed. In Wisconsin 11% of public arterial or collector roads are concrete (FHWA, 2018). At WisDOT when determining the appropriate pavement surface for a site, a 50-year LCCA is first performed (Harings, 2019). The lowest cost alternative is used, unless the results are within 5% at which point the engineer decides. Overall concrete typically has a higher initial cost, but at a certain depth of HMA, costs tend to equalize. In general in larger cities, where the AADT exceeds around 8,000, concrete is used (Harings, 2019) since concrete pavements also tend to have higher structural capacity (Kemp, 2019).

Although a project may initially use concrete pavement, by around the third rehabilitation it will be overlaid with asphalt typically due to joint failure (Harings, 2019). Wisconsin has not allowed studded tire use since the 1970s (Kemp, 2019), except for postal, buses, out-of-state and emergency vehicles in the winter (Wisconsin State Legislature 2017). WisDOT Pavement Engineer Harings noted he had never heard of rutting with concrete but longitudinal cracking does occur around the wheel path. There is also typically no premature rutting in their HMA.

Their concrete mix designs usually consist of a 6-sack concrete mix supplemented with fly ash, although silica fume and slag are allowed. Fly ash is usually added to decrease costs, with the added benefit of improved curing. The biggest problem reported regarding concrete pavements is the joints, which tend to deteriorate first. To limit panel cracking WisDOT has been reducing panel lengths from 18-22 feet to 15 feet. Overall Kemp noted they have had “pretty good success with concrete pavements.”

CHAPTER 3.0 SCREENING TESTS AND ANALYSIS

Initial screening tests to determine the fresh properties, compressive strength, and flexural strength of 10 mixes were conducted at the University of Alaska Fairbanks. Based on the results, four optimal mixes were determined. These mixes were then used for further performance testing at Missouri University of Science and Technology.

3.1 Materials and Specimen Preparation

3.1.1 Materials

Cementitious materials used include type I/II cement, class F fly ash, GGBFS, and BASF MasterLife SF100 silica fume. An air entraining admixture (AEA) BASF microair AE200 and HRWR BASF Glenium 1466 was also used. Aggregate used consisted of fine and intermediate-sized particles. Following ASTM C136, multiple sieve analyses were performed (Figures 3.1 and 3.2). The fineness moduli of the intermediate and fine aggregates were 6.0 and 3.0, respectively. Intermediate aggregate was washed over with a #200 sieve and oven dried overnight. The moisture content of the fine aggregate was measured regularly to maintain a consistent w/c ratio.

3.1.2 Mixes

Using the initial mix design (Table 3.1) the water content, air entrainment dosage, and aggregate ratios remained the same, but the SCMs and their respective contents were changed. The HRWR content was also altered depending on the batch to maintain workability. All mixes had a cement factor of 7.0 with a 0.331 w/c ratio. The original mix design was used in the field on the King Salmon Main Runway Rehabilitation project by Anchorage Sand and Gravel in King Salmon, Alaska in 2012.

In total 10 mixes were tested (Table 3.2). For silica fume, the equivalent dosage of either a full or

half 50-lb bag of silica fume per cubic yard concrete was used, equivalent to 3.8% or 7.6% of cementitious material by mass. The remaining cementitious material consisted of either 25% or 40% class F fly ash or GGBFS, henceforth referred to as slag.

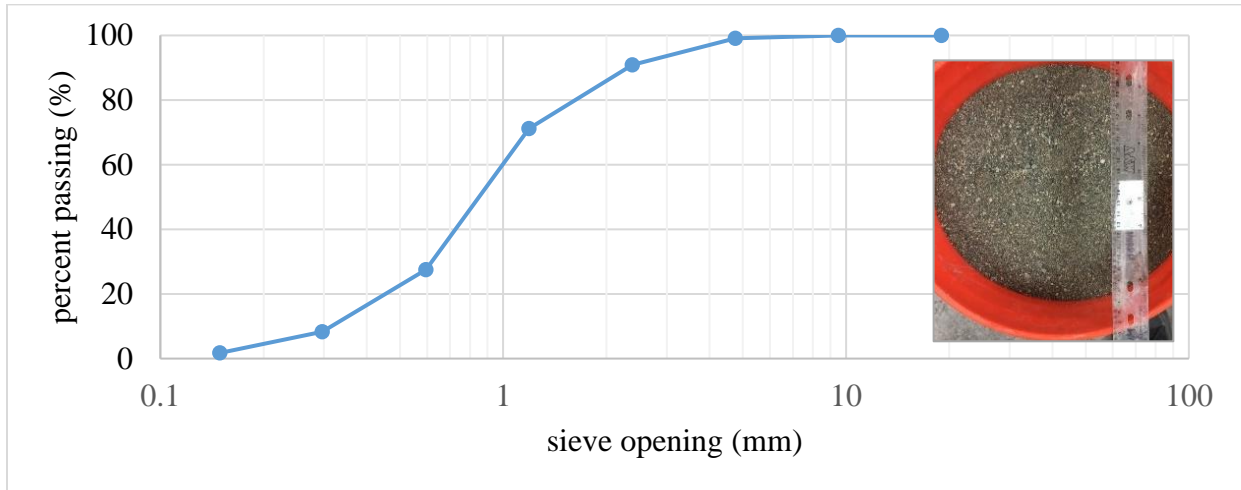


Figure 3.1 Alaska fine aggregate gradation chart

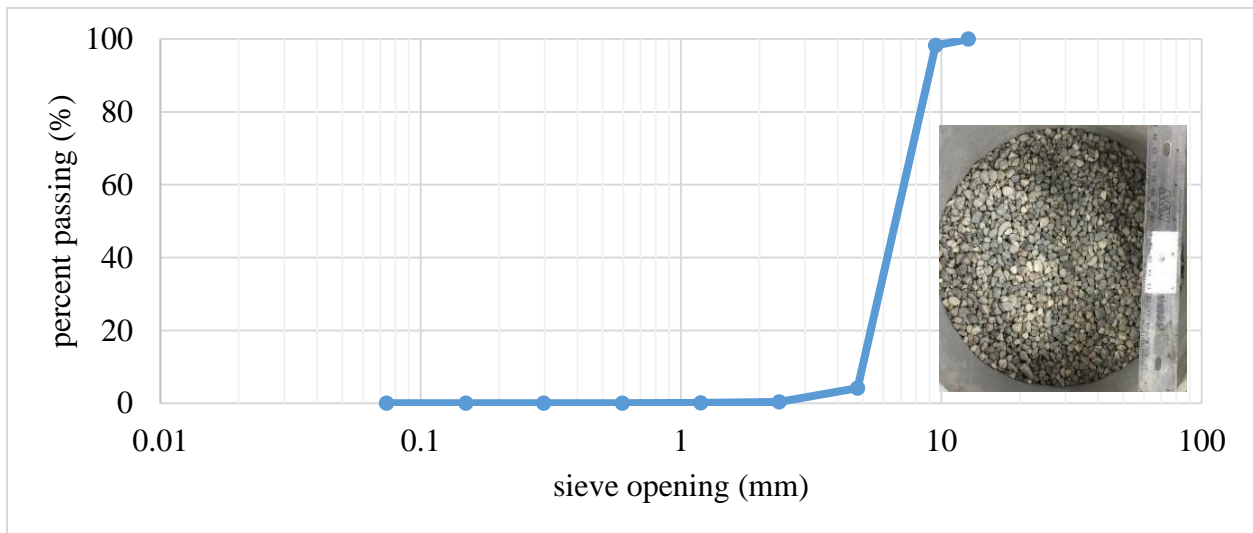


Figure 3.2 Alaska intermediate aggregate gradation chart

Table 3.1 Base mix design

Constituent	Quantity	Unit	Cementitious Material (% mass)
Type I Cement	611	lb	92
Silica fume	50	lb	8
Intermediate aggregate	1826	lb	
Fine aggregate	1248	lb	
Water	252.5	lb	
Air-entraining admixture (BASF AE200 microair)	14.8	mL	
High range water-reducing admixture	1956	mL	

Table 3.2 Total cementitious material percent composition for each screening test mix

Mix (No.)	Cement (%)	Silica fume (SF) (%)	Slag (SL) (%)	Class F fly ash (FA) (%)
1. SF8 (base)	92	8	0	0
2. SF4	96	4	0	0
3. SF4 SL38	58	4	38	0
4. SF4 FA24	72	4	0	24
5. SF8 SL37	55	8	37	0
6. SF4 SL24	72	4	24	0
7. SF4 FA38	58	4	0	38
8. SF8 FA37	55	8	0	37
9. SF8 SL23	69	8	23	0
10. SF8 FA23	69	8	0	23

3.1.3 Mixing

The same procedure was used for each batch. Aggregate was first mixed with 75% of the water for five minutes. Then the silica fume was added and mixed for five minutes, followed by the remaining cementitious material. The HRWR and the remaining 25% of the water was then added and mixed for two minutes, followed by the AEA for two minutes. Slump was then measured (Figure 3.3a). If workability was poor, additional HRWR was added to improve

workability. Batches, with the exception of a few smaller ones, were all made in the same mixer (Figure 3.3b). Once an appropriate slump was achieved, air content was measured (Figure 3.3c).

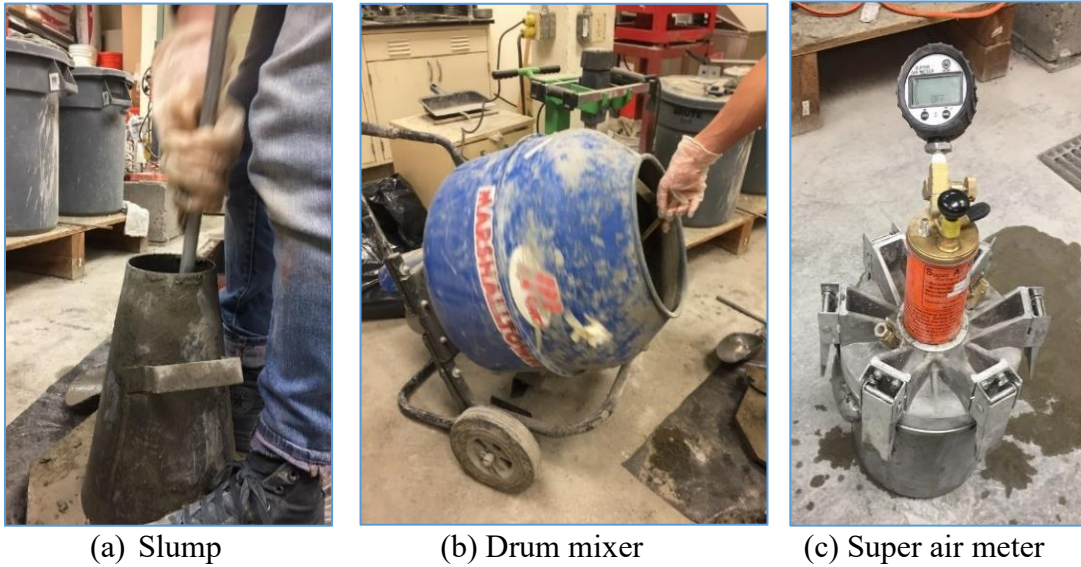


Figure 3.3 Mixing and testing concrete

3.1.4 Specimen Fabrications

After mixing and testing fresh properties of mixes, molds were filled per ASTM C192. Four by eight inch cylindrical molds were filled in two equal layers, rodded 25 times, and hit with an open palm 10-15 times after each layer. Excess concrete was struck off, smoothed, and covered with a lid. To fill the flexural strength molds, six by six by 21 inch beam molds were filled in two equal layers. After each layer, the concrete was rodded 60 times, and each side was tapped 15 times with a mallet. After filling, excess concrete was struck off and smoothed over (Figure 3.4a). Samples were then covered. The following day they were removed from the molds (Figure 3.4b), labeled, and placed in lime saturated water (Figure 3.4c).



(a) Finishing samples (b) Covering samples (c) Samples curing

Figure 3.4 Preparing samples

3.2 Testing Procedures

3.2.1 Workability and Air Content

ASTM C143 was followed for workability measurement. The mold was filled in three equal layers. After each layer, the mold was tamped 25 times. Excess cement was struck off, the mold removed, and the slump was measured.

To measure the air voids of the fresh cement, AASHTO method TP 118-17 was followed using a Super Air Meter (Figure 3.3c). The mold and instruments were wetted beforehand. Cement was then added in three equal layers. After each layer, the chamber was rodded 25 times and tapped 10-15 times with a mallet. Excess cement was then struck off, the lid was secured, and water was added through the petcocks. The pressure was then increased to 14.5, 30, and 45 psi before releasing the pressure and repeating. Afterwards concrete was disposed of.

3.2.2 Compressive and Flexural Testing

To measure compressive strength ASTM C39 was followed. Cylinders were loaded at 35

psi/second until failure (Figure 3.5a). For flexural testing, a modified ASTM C78 was used. The 14 day and 28 day beams for the control mix (SF8) were broken using a force method of 1800 pounds per minute. Because of safety concerns, the remaining beams were broken using a displacement method with a rate of 0.0002 inches per second (Figure 3.5b).



Figure 3.5 Compressive and flexural strength testing

3.3 Results

3.3.1 Workability

Despite adding additional HRWR to some mixes to maintain workability, workability still varied. As shown in Figure 3.6, workability decreased as the silica fume content increased. This is not surprising given silica fume's high surface area, which increases water demand (ACI, 2012). Al-Amoudi et al. (2011) also found the addition of silica fume, when compared to an all-

cement mix, required an increase in water to maintain similar workability, while Mazloom et al. (2004) found that as silica fume dosages increased to 15%, additional superplasticizer was needed to maintain workability. Research by El-Chabib and Syed (2012) on binary, ternary, and quaternary mixes containing fly ash, silica fume and slag also found mixes containing silica fume contents up to 10% improved compressive strength, but decreased workability. Wang and Li (2012) research had similar findings and found that a 12% silica fume content caused a 14% decrease in workability, but only minimal effects on workability when contents were less than 6%. The addition of fly ash also appears to improve workability while the addition of slag reduced workability, which aligns with the findings of other researchers (Figure 3.6) (Berndt, 2009; Hale et al., 2008). There was no correlation between 28 day compression strength and workability, but there was a weak significant correlation between 28 day flexural strength and workability ($R^2 = 0.45$, $P = 0.03$).

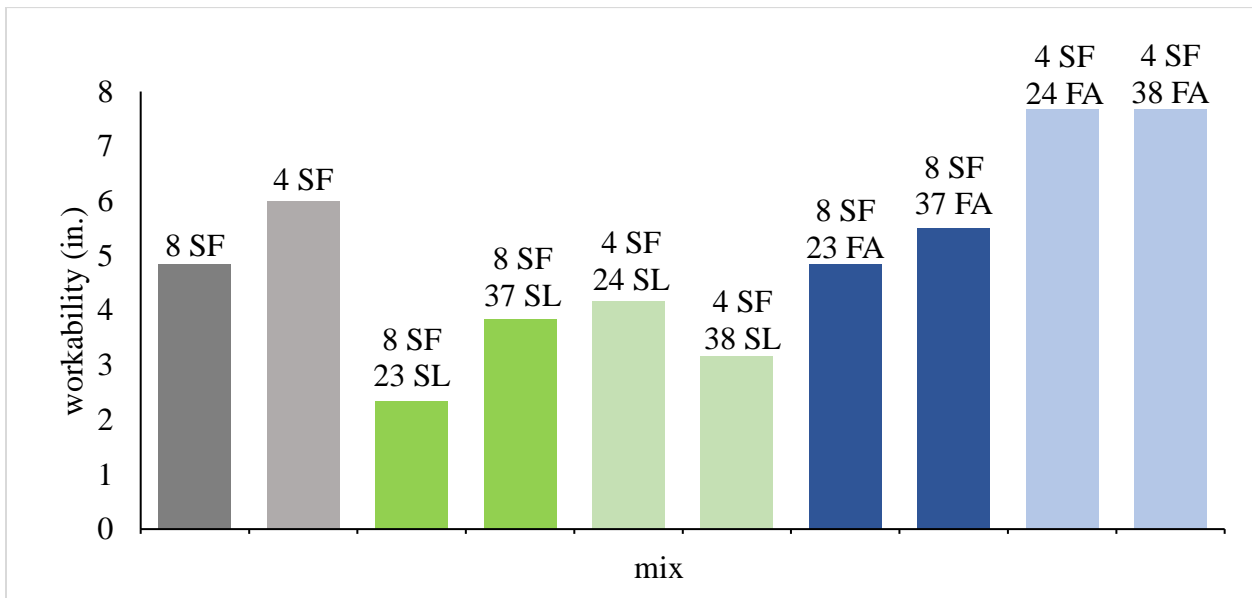


Figure 3.6 Workability of each screening mix

Other researchers found that as fly ash content increases in a mix, water demand is reduced (Naik and Ramme, 1989; Ravina and Mehta, 1986), due in part to the spherical shape of fly ash particles. Since the w/c ratio was consistent between mixes, with additional HRWR added only to improve workability, this may explain why the fly ash mixes would have higher workability than the control. Regarding slag, Sivasundaram and Malhotra (1992) found slag cement had reduced workability when compared to plain cement, while other researchers found that slag improved workability (Meusel and Rose, 1983; Oner et al., 2005).

3.3.2 Air Content

Overall fly ash mixes had the highest air content, while the slag mixes had the lowest air contents (Figure 3.7), which was consistent with the finding of Hale et al. (2008). The air content values of the SF8 SL23 and SF8 FA23 were not measured and were not included.

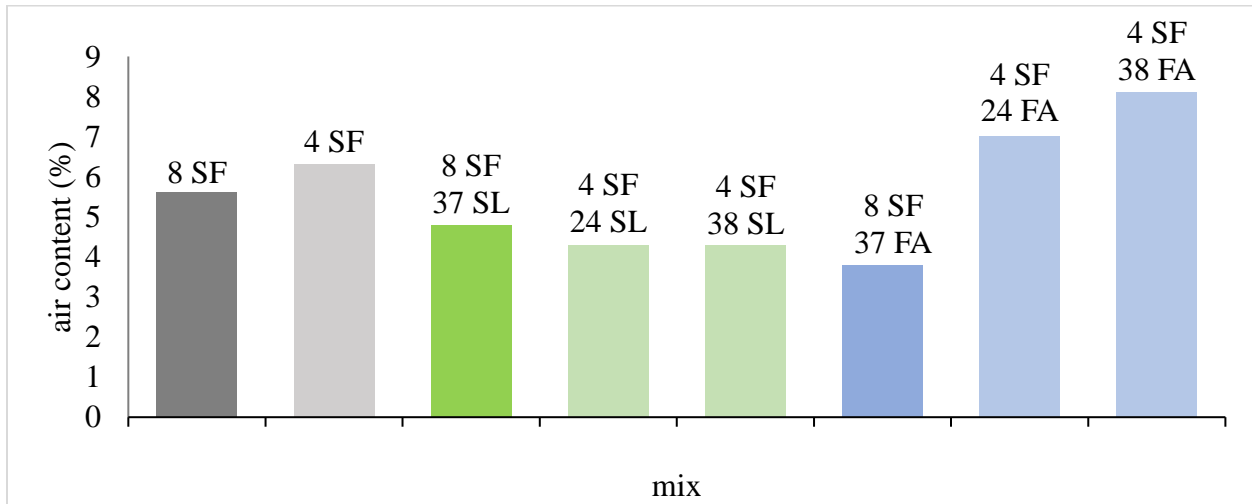


Figure 3.7 Air content of each screening mix

3.3.3 Compressive Strength

When averaging compressive strength of mixes containing either 4% or 8% silica fume, samples containing 8% silica fume had higher compressive strength than those with 4% at all ages

(Figure 3.8). Shannag (2000) tested compressive strength up to 56 days and also found a positive correlation between silica fume contents up to 15% and compressive strength. Bhanja and Sengupta (2005) found that optimum 28 day compressive strength could be achieved with a 15-25% silica fume content.

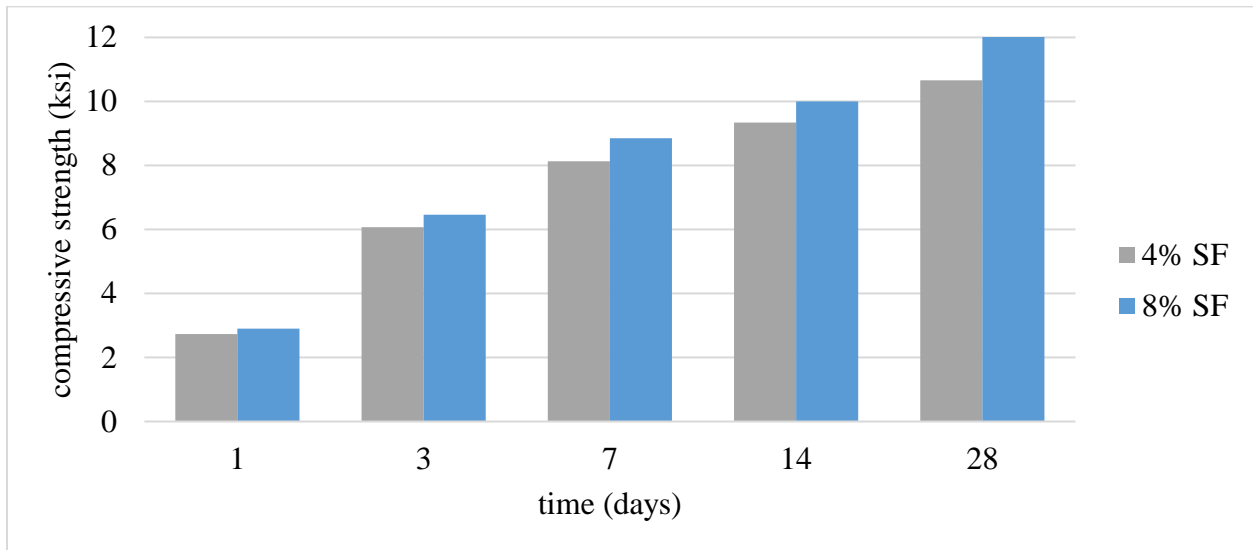


Figure 3.8 Compressive strength (ksi) vs. time (days) at 4% and 8% silica fume content

Regardless of silica fume content, the control mix had the highest compressive strength at one day (Figures 3.9 and 3.10). By three days, fly ash mixes had higher compressive strength than slag mixes with the same SCM content. By seven days, compressive strength of fly ash and slag were similar. By 14 days, mixes containing slag had higher compressive strength than fly ash mixes with the same SCM contents. This was inconsistent with Erdem and Kirca’s research (2008) on ternary blended concretes with silica fume and either class F fly ash, class C fly ash, or slag which found that for compressive strength measurements from three to 28 days, class C fly ash performed the best, followed by slag, and lastly class F fly ash. Research by Gesoglu (2009)

on self-compacting concretes measured the 28 day compressive strength of ternary and binary mixes containing silica fume, silica fume with fly ash, or silica fume with slag. They found the respective strengths of the mixes to be almost identical but also noted that mixes containing fly ash generally had lower compressive strength. Research by Hale et al. (2008) looked at the compressive strength of four mixes: a PCC cement, a 25% slag cement, a 15% type C fly ash cement, and a 25% slag with 15% fly ash cement and found the slag cement had the highest compressive strength at all ages from 3-90 days (Hale et al., 2008).

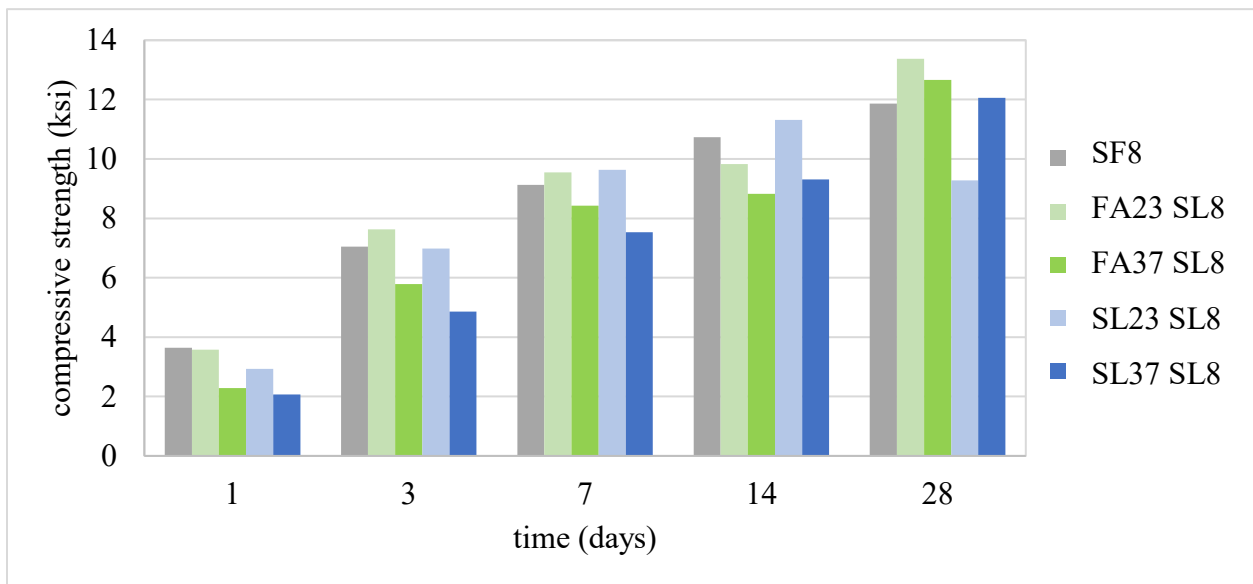


Figure 3.9 Compressive strength (ksi) of 8% silica fume mixes vs. time (days)

In addition, for almost all SCM mixes from one to 28 days, the mix containing the lower dosage of fly ash or slag had higher compressive strengths than those with higher doses. This does not align with Oner et al. (2005) which found 28 day compressive strength increased as fly ash content increased to 40%, but their samples did not contain silica fume. Yen et al. (2007) also tested fly ash mixes, these with a w/c ratio of 0.33, and found samples containing 15% fly ash had higher 28-364 day compressive strength over samples containing up to 30% fly ash.

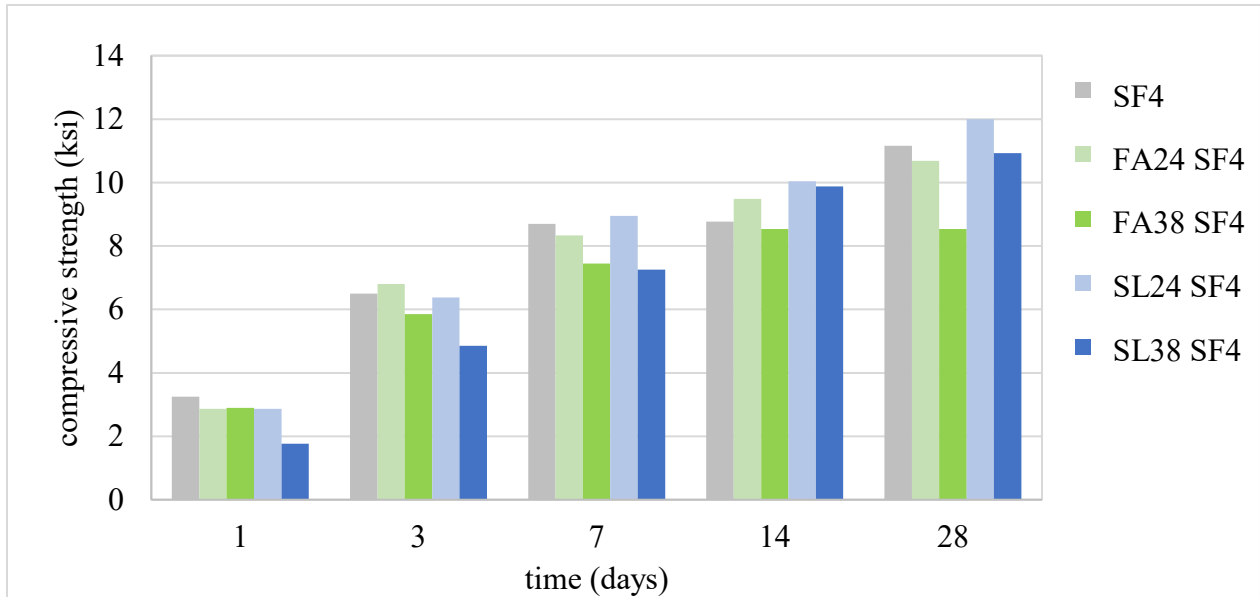


Figure 3.10 Compressive strength (ksi) of 4% silica fume mixes vs. time (days)

In addition, for almost all SCM mixes at ages up to 28 days, the mix containing the lower dosage of fly ash or slag had higher compressive strengths than those containing higher amounts. This does not align with Oner et al. (2005) which found that 28 day compressive strength increased as fly ash content increased up to 40%. Their samples did not contain silica fume. On the other hand, Yen et al. (2007) tested fly ash concretes with a w/c ratio of 0.33 and found that samples containing 15% fly ash had higher compressive strength at ages from 28-364 days over those samples containing up to 30% fly ash.

3.3.4 Flexural Strength

Regarding the effect of silica fume content on flexural strength at 7, 14, and 28 days, there seems to be no obvious trends (Figure 3.11). Bhanja and Sengupta (2005) found that at a w/c ratio of 0.34 the 28-day flexural strength of concrete samples increased as the silica fume content increased up to 10%, which is similar to the 28-day compressive strength findings presented

here. Yogendran et al. (1987) also found that 28-day flexural strength increased with an increasing silica fume content of up to 10%.

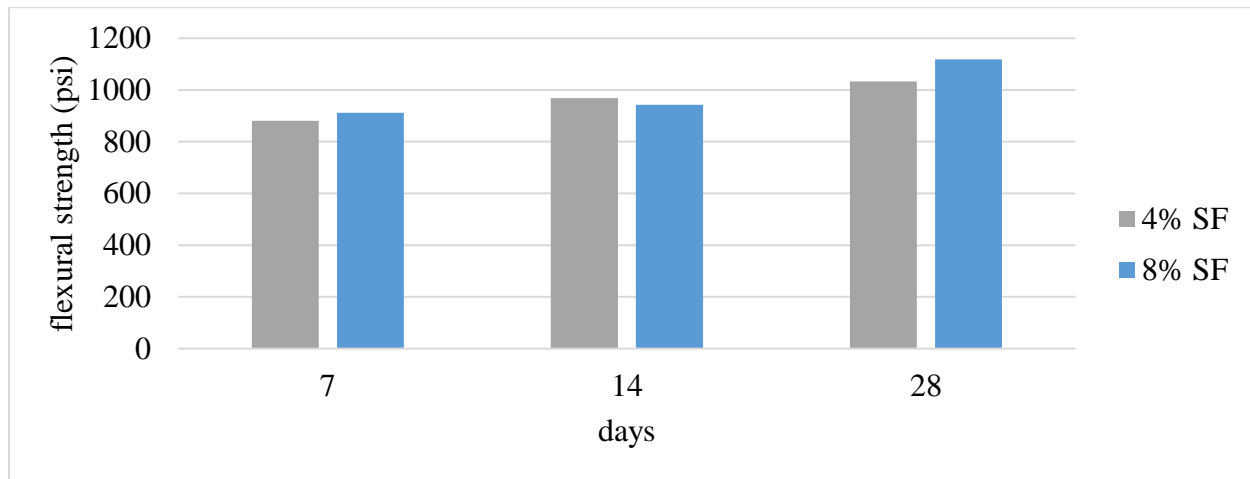


Figure 3.11 Average flexural strength of mixes and their silica fume content

Mixes containing 23-24% slag had the highest flexural strength at both silica fume contents (Figures 3.12 and 3.13). Lee and Yoon (2015), who tested binary and ternary mixes using fly ash and slag had different results and concluded that SCM type had no significant effect on flexural strength. Bharatkumar et al. (2001) also found that adding fly ash or slag did not significantly affect flexural strength, but did find a correlation between flexural and compressive strength.

3.4 Determining the Optimum Mix

Using the results obtained, an optimum mix for each parameter (e.g. 1 day compressive strength, 3 day compressive strength, etc.) was determined. This was first done using Minitab[®] Statistical Software Response Optimization tool (Minitab 2019), and later verified in Excel using special cubic models and desirability functions. Minitab is a statistical analysis program that has a function available to optimize mixes.

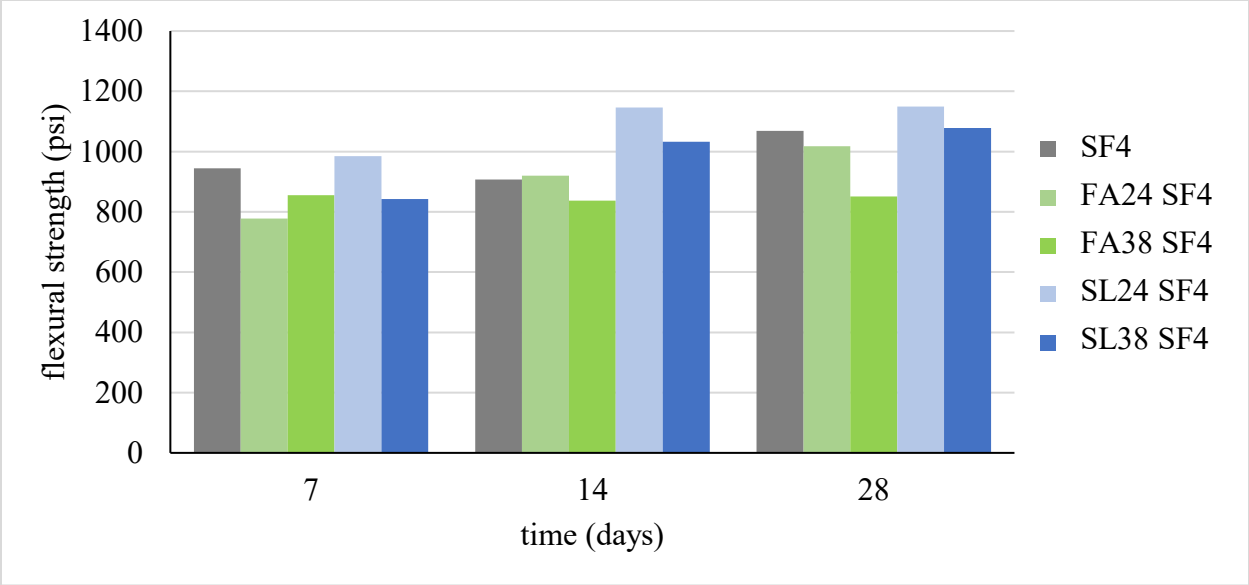


Figure 3.12 Flexural strength (psi) of mixes with 4% silica fume content vs. time (days)

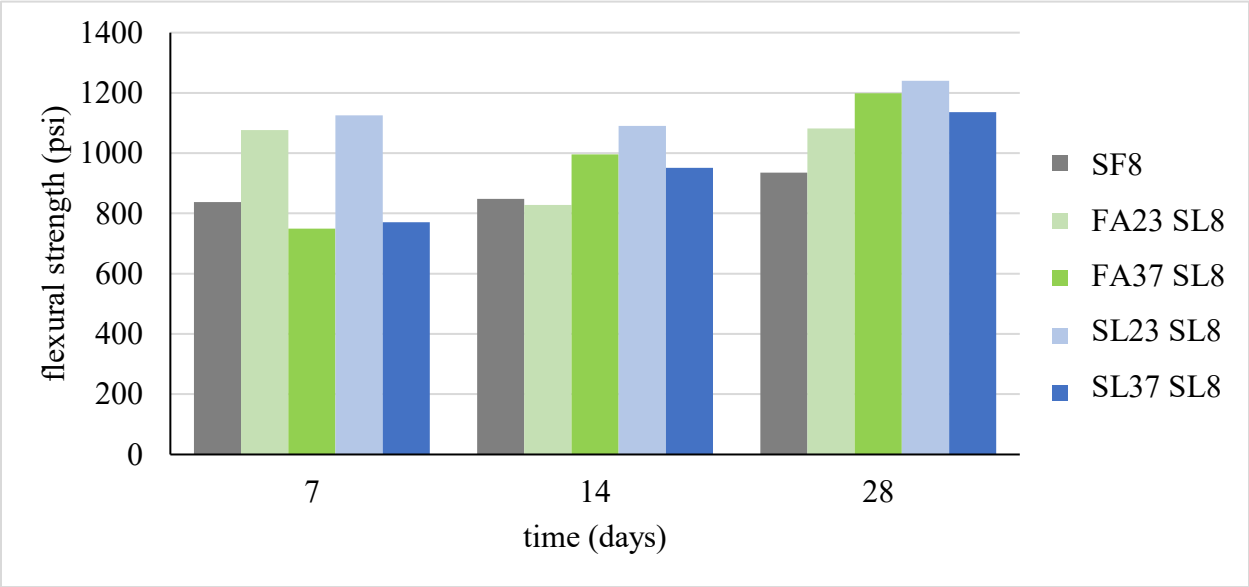


Figure 3.13 Flexural strength (psi) of mixes with 8% silica fume content vs. time (days)

3.4.1 Minitab Method

Using Minitab response optimization, slag, fly ash, silica fume, and cement contents were limited to the maximum and minimum quantities tested (Table 3.3). Following this, the

responses were modeled. These responses included workability; 1, 3, 7, 14 and 28 day compressive strength; and 7, 14 and 28 day flexural strength.

Table 3.3 Constraints used (% cementitious material)

constituent	Cement (%)	Silica fume (%)	GGBFS (%)	Fly ash (%)
lower limit	55	3.8	0	0
upper limit	96	7.6	3.8	3.8

Three models were investigated including linear (Equation 3.1), quadratic (Equation 3.2) and special cubic models (Equation 3.3). Linear models describe how each individual component affects the response. Quadratic models describe how two different components may affect each other and the response, and a special cubic describes how the combination of three components may affect an outcome. Other models were not used because modeling the effects of, say cement \times cement, is unrealistic and redundant. In these models, some relationships were not included. These include silica fume \times fly ash, slag \times fly ash, cement \times slag \times fly ash, and silica fume \times slag \times fly ash. In the first case, silica fume \times fly ash, this is due to multicollinearity. In the case of the latter three, the combination of slag and fly ash together were not tested, and therefore an appropriate coefficient for representing this relationship was not determined. The sum of squares (S), r-squared value (R^2) and P-value for each model and response are summarized in Table 3.4. Overall, it appeared the special cubic model resulted in the highest R^2 values. The association between the estimated and actual data was significant at the 0.05 level for all responses except 28 day flexural strength ($P = 0.06$), which was marginally statistically significant. Therefore, a special cubic model was used to model the data.

$$\text{response} = A(\text{cem}) + B(\text{sf}) + C(\text{fa}) + D(\text{sl}) \quad (\text{Equation 3.1})$$

$$\text{response} = A(\text{cem}) + B(\text{sf}) + C(\text{fa}) + D(\text{sl}) + E(\text{cem})(\text{sf}) + F(\text{cem})(\text{sl}) \quad (\text{Equation 3.2})$$

$$+ G(\text{cem})(\text{fa}) + H(\text{sf})(\text{sl})$$

$$\text{response} = A(\text{cem}) + B(\text{sf}) + C(\text{fa}) + D(\text{sl}) + E(\text{cem})(\text{sf}) \quad (\text{Equation 3.3})$$

$$+ F(\text{cem})(\text{sl}) + G(\text{cem})(\text{fa}) + H(\text{sf})(\text{sl})$$

$$+ I(\text{cem})(\text{sf})(\text{sl}) + J(\text{cem})(\text{sf})(\text{fa})$$

cem = cement, sf = silica fume, fa = fly ash, sl = slag

After determining the appropriate model, targets were set to maximize each response. These targets were set at 10% higher than the highest average mix measurement. For example, the SF8 mix had the highest average one-day compressive strength so 110% of its compressive strength was the target. The minimum value used was the lowest average measurement. Each response was set to maximize at these set targets except workability, which was set at six inches. The upper (target) and lower limits, weight, and importance of each response are summarized in Table 3.5. All responses were weighed equally at 1.0, but the importance factor, k , varied. Workability, flexural strength and compressive strength were considered of equal importance at 3.33. Therefore, for each compressive strength response (1 day, 3 day, etc.) the importance (k) was 0.67, and for each flexural strength response, the importance was 1.11. Minitab then determined the optimum mix to contain 12% slag, 4% silica fume and 1% fly ash (Figure 3.13).

3.4.2 Excel Method

Using the same constraints as those used in Minitab (Table 3.3), as well as a special cubic model, coefficients were determined for each parameter (Table 3.5). Another constraint was also added

which required the cement, silica fume, slag and fly ash to sum to 100%. Subsequently the same targets as used in Minitab (Table 3.6) were used to maximize the desirability of each response.

Table 3.4 Models fit for each response

Response	Model	S	R²	P-value
1 day compressive strength	linear	541	50.59	0.000
	quadratic	529	59.96	0.002
	special cubic	507	66.60	0.003
3 day compressive strength	linear	817	44.36	0.001
	quadratic	633	71.74	0.000
	special cubic	637	73.98	0.000
7 day compressive strength	linear	959	31.64	0.018
	quadratic	839	55.71	0.006
	special cubic	869	56.86	0.022
14 day compressive strength	linear	1050	27.69	0.035
	quadratic	940	51.02	0.015
	special cubic	957	53.85	0.036
28 day compressive strength	linear	1050	54.08	0.000
	quadratic	629	86.14	0.000
	special cubic	656	86.38	0.000
7 day flexural strength	linear	141	11.38	0.574
	quadratic	126	47.34	0.243
	special cubic	72	85.72	0.003
14 day flexural strength	linear	96	39.87	0.039
	quadratic	56	83.68	0.001
	special cubic	42	92.52	0.000
28 day flexural strength	linear	128	25.36	0.186
	quadratic	99	66.61	0.030
	special cubic	100	71.40	0.064
workability	linear	2	47.32	0.001
	quadratic	2	59.29	0.006
	special cubic	2	65.70	0.007

Table 3.5 Special cubic model coefficients for each response

Term	Compressive strength (days)					Flexural strength (days)			Slump
	1	3	7	14	28	7	14	28	
Cement (CEM)	1412	4914	7782	6938	11270	526	1229.4	1429	10.49
Silica fume (SF)	-432495	-298347	-134331	97290	283651	-164925	81067	68220	1009
Slag (SL)	-15473	-5407	-7835	22839	-1266	2417	-658	1572	-31.9
Fly ash (FA)	22104	4917	4245	-6534	-25697	9077	-3366	-3549	-39.5
CEM × SF	501296	358616	172912	-43531	-286215	183452	-91826	-79318	-1161
CEM × SL	22963	11744	19600	-12725	17182	-4287	3698	-1318	54.9
CEM × FA	-33563	-1580	-2946	29747	35454	-15566	6772	5457	101
SF × SL	606619	120262	-21029	-641665	-404447	80667	-103951	-115140	-208
CEM × SF × SL	-192406	379658	360476	776260	297396	192641	24627	91538	-1500
CEM × SF × FA	766740	585718	390542	-273278	-52043	327056	-135994	-79493	-2195

Table 3.6 Response limits and importance

Response	goal	lower limit	upper limit	target	weight	importance
1 day compressive	maximize	1764	-	3641	1.0	0.67
3 day compressive	maximize	4853	-	7626	1.0	0.67
7 day compressive	maximize	7250	-	9632	1.0	0.67
14 day compressive	maximize	8533	-	11316	1.0	0.67
28 day compressive	maximize	8535	-	13371	1.0	0.67
7 day flexural strength	maximize	750	-	1126	1.0	1.11
14 day flexural strength	maximize	828	-	1147	1.0	1.11
28 day flexural strength	maximize	852	-	1240	1.0	1.11
workability	target	2.3	7.7	6.0	1.0	3.33

This can be done using either using an equation to reach a certain target (Equation 3.4), maximize the response (Equation 3.5), or minimize the response (Equation 3.6) (Derringer and Suich, 1980). Since the aim of the optimum mix was to maximize the strength at all ages, Equation 3.6 was used for all responses except slump (workability). For workability, Equation 3.4 was used to reach a target of six inches.

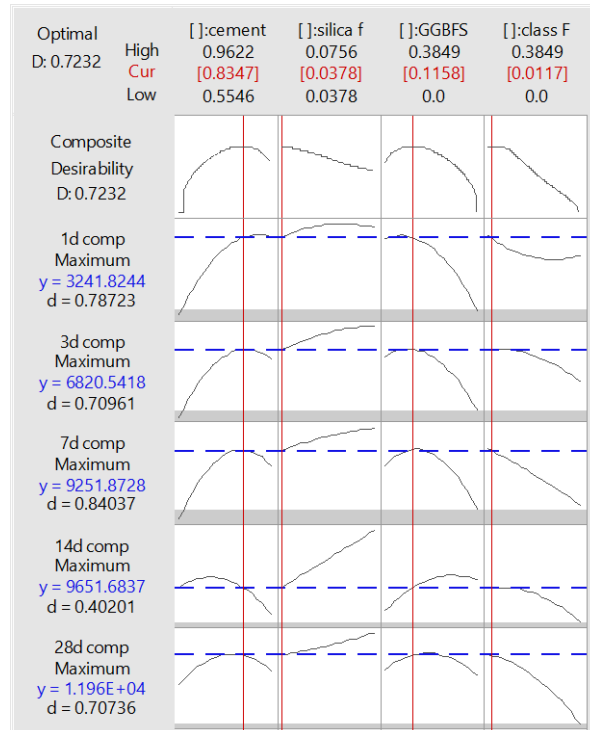


Figure 3.14 Optimum mix as determined by Response Optimizer for Mix on Minitab

$$d(x) = \begin{cases} 0 & \text{if } x < L \\ \left(\frac{x-L}{T-L}\right)^w & \text{if } L \leq x \leq T \\ \left(\frac{x-U}{T-U}\right)^w & \text{if } T \leq x \leq U \\ 0 & \text{if } x > U \end{cases} \quad \text{(Equation 3.4)}$$

$$d(x) = \begin{cases} 0 & \text{if } x < L \\ \left(\frac{x-L}{T-L}\right)^w & \text{if } L \leq x \leq T \\ 1 & \text{if } x > T \end{cases} \quad \text{(Equation 3.5)}$$

$$d(x) = \begin{cases} 1.0 & \text{if } x < T \\ \left(\frac{x-U}{T-U}\right)^w & \text{if } T \leq x \leq U \\ 1 & \text{if } x > U \end{cases} \quad \text{(Equation 3.6)}$$

L = lower bound U = upper bound T = target W = weight

Following this, each response was assigned an importance value and each response's respective desirability was used to determine the overall desirability the mix will provide (Equation 3.7) (Derringer and Suich, 1980; Aksezer, 2008). Excel solver was then used to maximize the desirability within the given limits. The optimum mix determined using Excel was found to be almost identical to the mix determined using Minitab (Tables 3.7 and 3.8).

$$D = (d_1(x_1)^{k_1} \times d_2(x_2)^{k_2} \times \dots \times d_n(x_n)^{k_n})^{\frac{1}{\sum_i k_i}} \quad \text{(Equation 3.7)}$$

Table 3.7 Excel versus Minitab optimum mix

Method	Desirability	Cement	Silica fume	GGBFS	Class F fly ash
Excel	0.7233	0.8355	0.0378	0.1159	0.0109
Minitab	0.7232	0.8347	0.0378	0.1158	0.0117

Table 3.8 Predicted value and desirability for each response in the optimum mix

Response	Excel			Minitab		
	Predicted		Desirability	Predicted		Desirability
1 day compressive strength	3245	psi	0.79	3242	psi	0.79
3 day compressive strength	6820	psi	0.71	6821	psi	0.71
7 day compressive strength	9255	psi	0.84	9252	psi	0.84
14 day compressive strength	9650	psi	0.40	9652	psi	0.40
28 day compressive strength	11958	psi	0.71	11956	psi	0.71
7 day flexural strength	992	psi	0.64	991	psi	0.64
14 day flexural strength	1086	psi	0.81	1086	psi	0.81
28 day flexural strength	1137	psi	0.73	1136	psi	0.73
workability	5.2	in.	0.78	5.2	in.	0.78

3.4.3 Results

This method was repeated for determining three other mixes: (1) for optimal workability, (2) for optimal one to 28 day compressive strength, and (3) for seven to 28 day optimal flexural strength. In case (1) workability was the only response used. In case (2) all five compressive

responses were used with equivalent importance assigned while in case (3) all three flexural strength responses were used with equivalent importance assigned. These results, along with the overall optimum mix and the original control were then used for further testing (Table 3.9).

Table 3.9 Mixes determined for performance testing

Name	Silica Fume (%)	Slag (%)	Fly Ash (%)	Cement (%)
Control (SF8)	8	0	0	92
Optimal flexural strength (SL22 SF8)	8	22	0	70
Optimal flexural, compressive, and workability (SL12 SF4 FA1)	4	12	1	83
Optimal compressive (SL8 SF8 FA3)	8	8	3	81
Optimal workability (FA31 SF4)	4	0	31	65

Other researchers also found that a primarily slag and silica fume mix would provide an optimal mix for concrete pavements. For example Scholz and Keshari (2010) developed an abrasion-resistant mix using silica fume, fly ash, and slag. They found a slag and silica fume mix had better durability, compressive strength and abrasion resistance over that of fly ash and silica fume mixes. Gesoglu et al. (2009) tested 22 binary, ternary, and quaternary mixes containing silica fume, slag and fly ash and concluded an optimum mix would contain primarily silica fume and slag. The optimum mix they determined contained 44% slag, 1% fly ash, and 14% silica fume.

CHAPTER 4.0 PERFORMANCE TESTS AND RESULTS

After determining the optimum mix designs, subsequent performance tests were conducted on these mixes to ascertain their mechanical and durability properties. Tests included measuring free shrinkage, abrasion resistance, compressive strength, freeze-thaw resistance, deicer scaling resistance and chloride ion penetration.

4.1 Materials and Specimen Preparation

4.1.1 Materials

For cementitious materials, Type I cement sourced from Missouri was used. The same silica fume, fly ash, and slag used during the screening tests were used. The same AEA was used, but the HRWR used was Glenium 7500. Similar aggregates to those used for the screening tests were used. The fineness moduli of the fine aggregate and intermediate aggregate were 3.0 and 5.8, respectively (Figures 4.1 and 4.2).

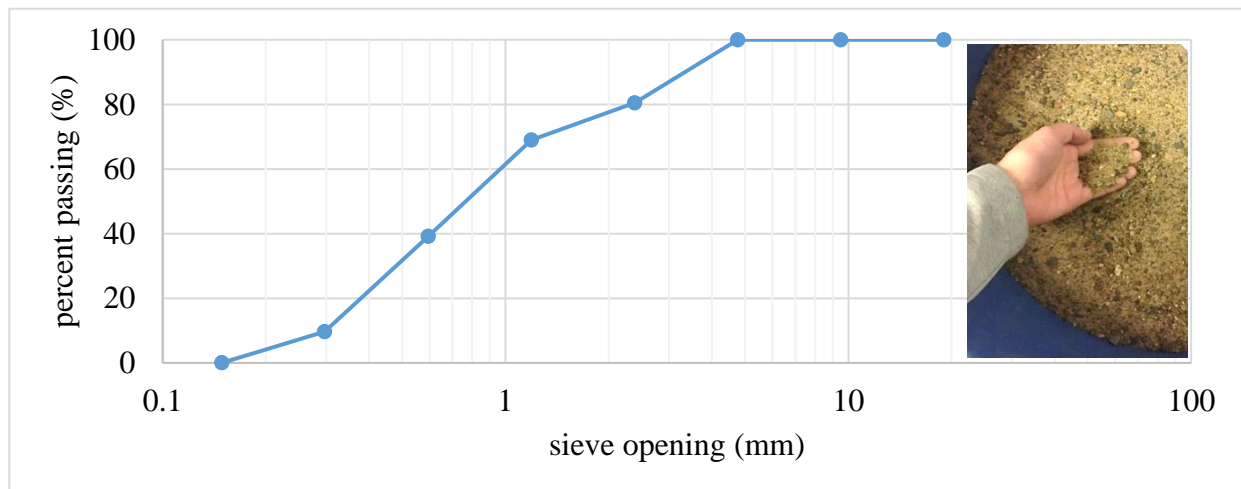


Figure 4.1 Missouri fine aggregate gradation chart

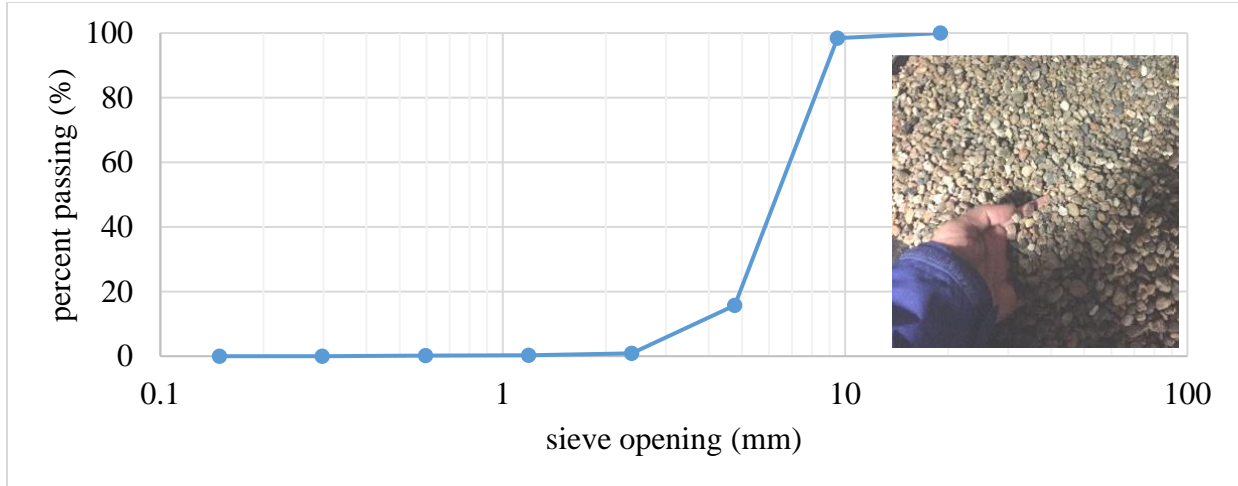


Figure 4.2 Missouri intermediate aggregate gradation chart

4.1.2 Mixes

As mentioned previously, five mixes were tested (Table 4.1). Similar to the screening mixes, the water content, air entrainment dosage, and aggregate ratios remained the same for all mixes, but the cementitious material dosages changed. The HRWR dosage was also altered depending on the batch to improve workability. These mixes represented the optimal mixes determined through data analysis from the screening tests results.

Table 4.1 Cementitious material percent composition for the optimal and control mixes

No.	Mix	Cement (%)	Silica Fume (%)	Slag (%)	Class F Fly Ash (%)
1	Control (SF8)	92	8	0	0
2	Optimal flexural strength (SL22 SF8)	70	8	22	0
3	Optimal flexural, compressive, and workability (SL12 SF4 FA1)	83	4	12	1
4	Optimal workability (FA31 SF4)	65	4	0	31
5	Optimal compressive (SL8 SF8 FA3)	81	8	8	3

4.1.3 Mixing and Specimen Fabrications

For the performance tests, the mixing method was identical to the screening test mixing method, with a few exceptions. Instead of adding silica fume before the other cementitious materials, silica fume was added at the same time as the other cementitious materials. In addition, air entrainment was added at the same time as the water and aggregate at the beginning of mixing, instead of adding near the end of mixing. Similar to the screening test specimen fabrications, after the fresh concrete was prepared the air content and workability were measured (Figure 4.3). Subsequently, molds were filled in two layers and vibrated. After filling, molds were covered with an impermeable plastic sheet. The following day samples were then demolded and placed in lime-saturated water in temperature-controlled curing baths.

4.2 Testing Procedures

4.2.1 Properties of Fresh Concrete

For workability ASTM C143 standard (2015a) was followed, same as during the screening tests. To measure the air voids of the fresh cement, ASTM method C231 (2017b) was followed (Figure 4.4). For this test, the air meter and lid were first wetted. Then the meter was filled by thirds with concrete. After each third, the concrete was rodded 25 times and the sides tapped 10-15 times with a mallet. Excess concrete was struck off, edges were wiped down, and the lid was attached and sealed shut. Water was then added through one petcock until clear water and no bubbles emerged from the opposite petcock. The air meter was then pressurized by pumping the knob to the designated pressure. The petcocks were then closed and the lever pressed. The vessel was hit once with a hammer and then the air content was read from the gauge.



(a) Slump and air meter equipment



(b) Molds being finished



(c) Unmolding cylinders



(d) Samples wet curing

Figure 4.3 Sample preparation



Figure 4.4 Air meter

4.2.2 Mechanical Properties

For compressive strength ASTM C39 (2018) was followed. Samples were crushed at a rate of 35 pounds per square inch per second. As for shrinkage ASTM standard C157 (2017a) was followed. Shrinkage samples were demolded approximately 24 hours after mixing, measured, and then cured for 28 days in a temperature-controlled water bath. After 28 days samples were measured again and left at 50% humidity at 23°C and measured daily for 28 days (Figure 4.5).



(a) Shrinkage molds (b) Measuring sample (c) Samples

Figure 4.5 Measuring shrinkage

4.2.3 Durability

4.2.3.1 Abrasion Resistance

Two methods were used to measure abrasion resistance. ASTM C944 measured abrasion resistance through mass loss while the second, measured resistance through volume loss.

ASTM C944 Test

For measuring abrasion resistance by mass loss, a modified ASTM C944 method (2012b) was followed. ASTM C944 requires the rotating-cutter drill press to spin at a rate of 200 revolutions per minute (rpms), but the press used only could rotate at 150 or 300 rpms, so 150 rpms was

used. A 22-pound force was applied for two minutes in four sections of the samples (Figure 4.6a). Mass loss was measured after each two-minute period (Figure 4.6b).



(a) Applying force to sample (b) Measuring mass loss

Figure 4.6 Testing abrasion by mass loss

Abrasion by Studs, Method A: Prall Method

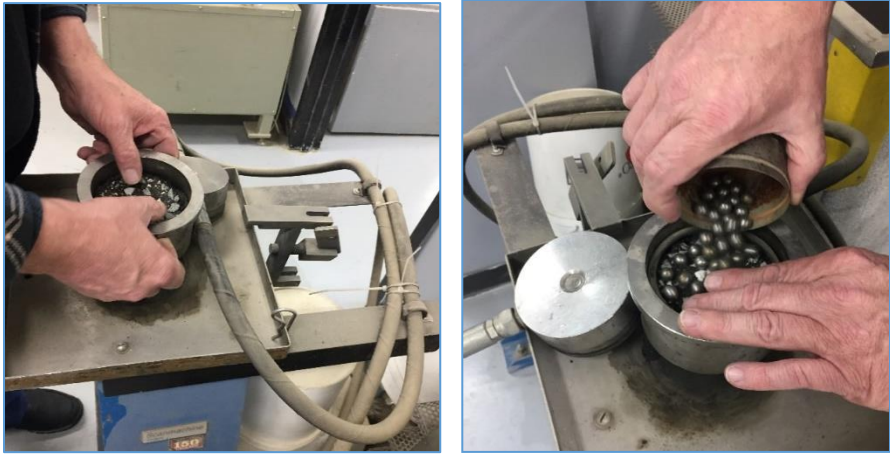
Abrasion resistance was also measured through volume loss using the Nordic Prall testing apparatus and the Abrasion by Studs, Method A: Prall Method standard (CEN WG1 Bituminous Materials, 1997). To prepare samples for this test after batching, four by eight inch cylindrical concrete samples were cured for 28 days and sent to the Alaska DOT&PF Southcoast Materials Lab. Upon arrival, samples were then cut into 100 mm diameter by 30 mm long disks and brought to a temperature of 5°C. Samples were then weighed and placed in the Prall machine (Figure 4.7). In the machine, samples were exposed to cooling water at a rate of two liters per minute, and worn for 15 minutes by 40 steel spheres at a rate of 950 revolutions per minute. The loss in volume before and after testing, referred to as the abrasion value, was measured. Two

samples were tested for each mix. The volume loss per sample was then used to determine the wear resistance (Table 4.2).



(a) Prall test setup

(b) Temperature controls



(c) Setting asphalt sample in chamber

(d) Adding steel spheres

Figure 4.7 Nordic Prall Test

Table 4.2 Prall results interpretation

Volume loss (cm ³)	Wear resistance
<20	Very good
20-29	Good
30-39	Satisfactory
40-50	Less satisfactory
>50	Poor

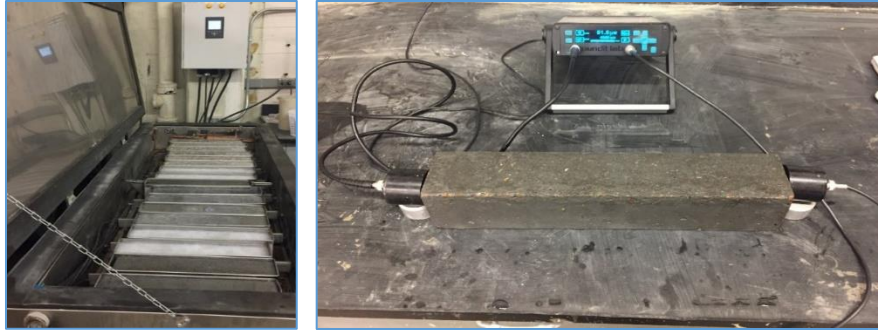
4.2.3.2 Freeze-Thaw Resistance

To measure the freeze-thaw resistance of samples, ASTM C666 (2015b) was followed. After curing in a water bath for 14 days each sample's length and mass was measured, as well as the ultrasonic pulse velocity. This velocity was measured using a PROCEQ ultrasound with a frequency of 54 Hz (Figure 4.8b). Samples were kept in a temperature-controlled cabinet (Figure 4.8a) which exposed samples to freezing temperatures for four hours, followed by two hours of thawing. After every 18 cycles each sample's mass, length and the ultrasonic pulse velocity was measured again. Originally, it was planned to expose the samples to 300 cycles, but due to time constraints, samples were only exposed to 180 cycles. To calculate the relative dynamic modulus of elasticity (RDME), Equation 4.1 was used. In this, v_0 is the initial ultrasonic pulse velocity and v_n is the ultrasonic pulse velocity at n cycles. The durability factor (DF) for each mix was also determined, using Equation 4.2.

In this equation n_f is the cycles the $RDME_f$ represents. The $RDME_f$ represents either the RDME once it reaches 60% or lower, or the RDME after 180 cycles, whichever occurs sooner. A higher durability factor suggests the sample has high resistance to freeze-thaw cycles. A lower durability factor suggests the sample's durability is low, and degraded quickly after many freeze-thaw cycles. The durability factor ranges from 0% to 100%.

$$RDME (\%) = \frac{v_0^2}{v_n^2} \quad (\text{Equation 4.1})$$

$$DF = RDME_f \times n_f / (300 \text{ cycles}) \quad (\text{Equation 4.2})$$



(a) Freeze-thaw cabinet (b) Measuring frequency

Figure 4.8 Freeze-thaw testing

4.2.3.3 Scaling Resistance of Samples Exposed to Deicing Chemicals

For measuring the scaling and deicing resistance of samples, ASTM C672 (2012a) was followed. Samples were cured in a water bath for 14 days and then in air for 14 days. Then the top edges were taped and caulked using waterproof silicone to provide a waterproof boundary (Figure 4.9a). A 4% calcium chloride (CaCl_2) solution was then applied to the sample's surface at a ¼ inch depth (Figure 4.9b) and samples were placed in the deicing chambers. The chamber was calibrated to expose samples to freezing temperatures for 16 hours and then 23°C for eight hours daily. Every five days the solution was replaced, samples were photographed, and the condition of their surface was rated 0-5 as per ASTM C672 ratings (Table 4.3).



(a) Preparing samples (b) Replacing salt solution on samples

Figure 4.9 Preparing and testing deicing samples

Table 4.3 ASTM C672 sample degradation ratings

Rating	Condition of Surface
0	No scaling
1	Very slight scaling (3 mm [1/8 in.] depth, max, no coarse aggregate visible)
2	Slight to moderate scaling
3	Moderate scaling (some coarse aggregate visible)
4	Moderate to severe scaling
5	Severe scaling (coarse aggregate visible over entire surface)

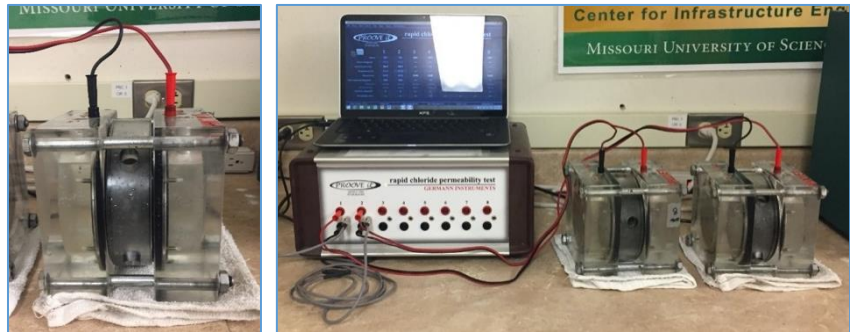
4.2.3.4 Chloride Ion Penetration Resistance

For chloride ion penetration ASTM C1202 (2019) was followed. First four by eight inch cylindrical samples were wet cured for 28 days. Samples were then cut into 50 mm disks using a water saw (Figure 4.10a) and grinded smooth. Next, samples were placed in a desiccator for three hours at a 50 mm Hg pressure (Figure 4.10b). With the vacuum pump still on water was added through a stopcock until samples were covered. Samples were then left submerged under pressure for an hour. Following this, the pump was turned off and samples were soaked for 18 hours. Samples were then placed in the testing chamber (Figure 4.10c) and each side was filled with either a 3.0% NaCl or 0.3 N NaOH solution. A 60 Volt electrical current was then applied across the sample for six hours (Figure 4.10d). Afterwards, the current versus time was plotted and a curve was drawn. The area under the curve was then integrated to determine the coulombs passed. Based on this, the penetrability was determined (Table 4.4).



(a) Cutting samples

(b) Samples in dessicator



(c) Sample in chamber

(d) Testing sample

Figure 4.10 Testing chloride ion penetration

Table 4.4 Chloride ion penetrability based on charge passed (ASTM 1202, 2019)

Charge passed (Coulombs)	Chloride Ion Penetrability
>4,000	High
2,000-4,000	Moderate
1,000-2,000	Low
100-1,000	Very Low
<100	Negligible

4.3 Results

4.3.1 Properties of Fresh Concrete

Workability varied widely from 1½ to 9¾ inches while the air content varied between 3-5% (Table 4.5). As predicted, the optimum workability mix, which contained 31% fly ash had the highest workability and air content of the mixes. This corroborates with research by Hale et al.

(2008) which found that fly ash mixes had higher slump and air content than slag mixes.

4.3.2 Mechanical Properties

4.3.2.1 Compressive Strength

By 28 days, the compressive strength of the control was the highest, followed by the SL8 SF8 FA3 mix, the SL22 SF8, FA31 SF4 and SL12 SF4 FA1 mixes (Table 4.6).

Table 4.5 Workability and air content of optimum and control mixes

Mix	Workability (in.)	Air content (%)
Control (SF8)	8.00	5.5
Optimal flexural strength (SL22 SF8)	9.50	3.4
Optimal all (SL12 SF4 FA1)	1.50	4.5
Optimal compressive (SL8 SF8 FA3)	3.00	5.3
Optimal workability (FA31 SF4)	9.75	5.6

Table 4.6 Compressive strength of optimum mixes

Mix	Compressive strength (psi)				
	1 day	3 days	7 days	14 days	28 days
Control (SF8)	3870	5920	6930	7360	7950
Optimal flexural strength (SL22 SF8)	3280	5960	7980	7300	7270
Optimal all (SL12 SF4 FA1)	4240	6180	6920	6670	6840
Optimal compressive (SL8 SF8 FA3)	3810	6230	8140	8340	7640
Optimal workability (FA31 SF4)	3700	5520	6370	6930	7210

4.3.2.2 Drying Shrinkage

As shown below in Figure 4.11, the FA31 SF4 mix had almost no length change, expanding 0.006%. The other mixes had a 0.02% to 0.03% length decrease (Table 4.7). Akkaya et al.

(2007) found that when comparing an all-cement mix to a ternary 20% class F fly ash and 8% silica fume mix, the ternary mix had higher drying shrinkage and lower autogenous shrinkage.

The drying shrinkage results presented here have similar findings when comparing the control

and fly ash mixes. Since the volume of cement paste is consistent between mixes, the drying shrinkage of mixes containing GGBFS should be similar to the control (Hooton, 2000). Research comparing all-cement mixes to those containing 5% and 15% silica fume found the addition of silica fume reduced drying shrinkage by 29% and 35% (Güneyisi et al., 2012). Hale et al. (2008) measured shrinkage over 90 days and found the addition of slag reduced shrinkage while fly ash mixes had similar shrinkage to the all-cement control mix. Similarly, Mokarem et al. (2005) tested binary mixes and found fly ash mixes had higher drying shrinkage over those of silica fume or slag. They suggested the 28-day length change for concrete mixes containing SCMs should be limited to 0.04%, which all the mixes presented here adhere to (Table 4.7).

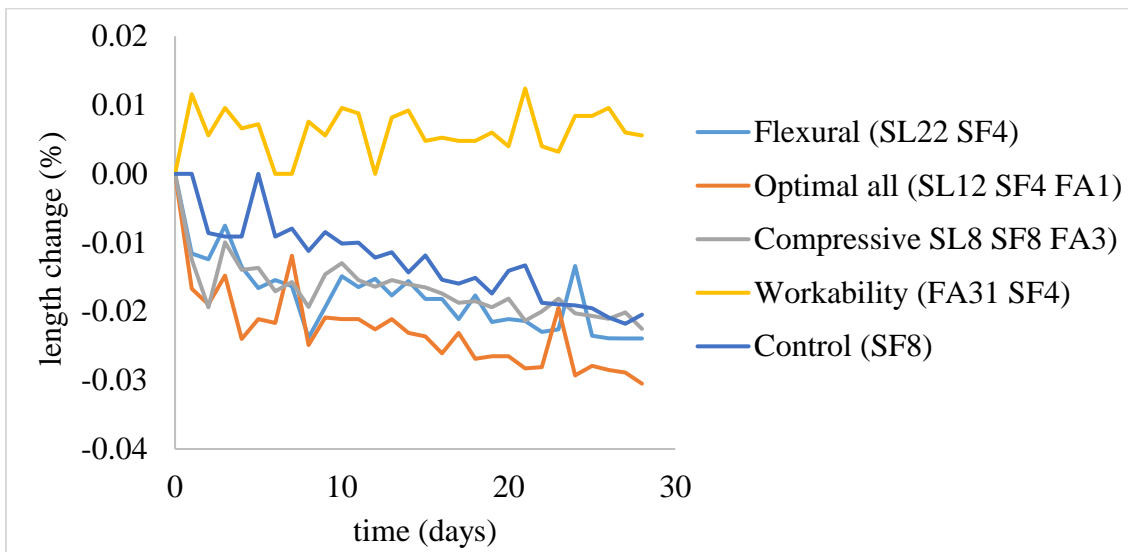


Figure 4.11 Time (days) vs. length change (%)

Table 4.7 28 day shrinkage per mix

Mix	28-day length change (%)
Control (SF8)	-0.020
Flexural (SL22 SF8)	-0.024
Optimal all (SL12 SF4 FA1)	-0.031
Compressive (SL8 SF8 FA3)	-0.023
Workability (FA31 SF4)	0.006

4.3.3 Durability of Hardened Concrete

4.3.3.1 Abrasion Resistance

ASTM C944 Test

For abrasion resistance, generally as the SCM content increased, the mass loss decreased (Figure 4.12) with the SF4 mix having the highest mass loss and the SL22 SF8 and FA31 SF4 mixes having the lowest mass loss. Each mix's mass loss can also be partially attributed to the higher packing density in mixes containing SCMs as well as the late-age strength-contributing pozzolanic reactions between the silica in the SCMs and the available CH. Langan et al. (1990); Rashad et al. (2014); and Atiş (2002) all found that generally when adding SCMs to concrete mixes, as compressive strength increases, abrasion resistance increases. Rashad et al. (2014) measured abrasion resistance in wear loss and found that as fly ash content increases to 70% in samples aged 28 to 180 days, abrasion resistance was reduced. On the converse in the data presented here, the fly ash mix actually had the lowest mass loss. This data does align with Atiş (2002) findings though. Atiş (2002) replaced cement with 50% and 70% fly ash and measured abrasion resistance in samples aged three days to three months and found that fly ash mixes had improved abrasion resistance over the all-cement mixes. Regarding the effects of slag, Fernandez and Malhotra (1990) measured the wear depth at 120 days of binary mixes containing up to 50% slag replacement and found the addition of slag reduced abrasion resistance, which does not align with this study's findings.

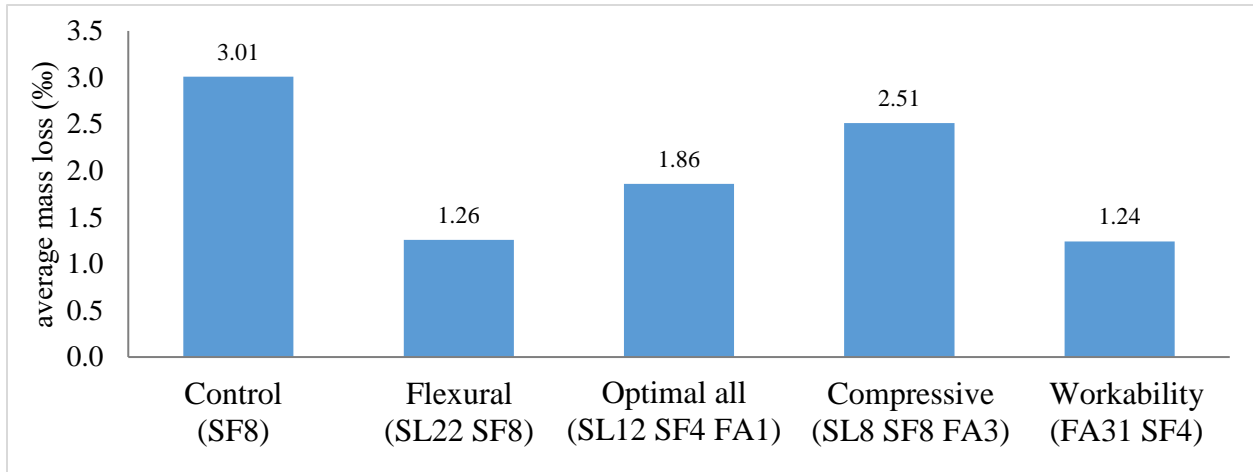


Figure 4.12 Mass loss of mixes due to abrasion testing

Abrasion by Studs, Method A: Prall Method

Of the five mixes tested, only the quaternary SL12 SF4 FA1 and SL8 SF8 FA3 mixes performed satisfactory, according to the Nordic Classification (Table 4.2). The performance of the other three mixes were less satisfactory (Table 4.8 and Figure 4.13). These classifications are dependent on the volume loss, so if there is high Prall-loss of over 40 or 50 cm³, the sample will be designated as less satisfactory or poor, respectively. Work done by Gartin and Saboundjian (2005) correlating Alaskan pavement rutting rates and their respective Prall values found an R² value of 0.933, suggesting a Prall test value is indicative of field performance. Scholz and Keshari (2010) also conducted Prall tests on high strength concrete mixes. Their results varied from 18.0 for a mix with a 13,600 psi 28 day compressive strength to 49.1 to their control mix which had a 7,860 psi 28 day compressive strength. In this study mixes had 28-day compressive strengths of 6,000 to 8,000 psi at 28 days, which if 28-day compressive strength is indicative of abrasion resistance, is reasonable. The Southcoast Alaska DOT&PF materials lab, after testing these samples noted that although a skid resistant calcined bauxite aggregate was used, the

aggregate was very small which resulted in a high paste surface area which eroded and released the aggregate particles. This may have contributed to the low test results (Bowthorpe, 2019).

Table 4.8 Prall test results

Mix	Prall-loss (cm ³)	Nordic Classification
SL8	45.3	Less satisfactory
SL22 SF8	43.2	Less satisfactory
SL12 SF4 FA1	37.3	Satisfactory
SL8 SF8 FA3	39.4	Satisfactory
FA31 SF4	49.5	Less satisfactory



Figure 4.13 Prall samples after testing (Bowthorpe, 2019)

4.3.3.2 Scaling Resistance after Exposure to Deicing Chemicals

Overall, all the mixes performed poorly with visual ratings of four to five after 50 days of exposure to a CaCl₂ solution and daily freeze-thaw cycles. These visual ratings were based on the ASTM C672 standard (Table 4.3). The SF4 and SL12 SF4 FA1 mixes performed the worst with severe surface scaling and a visual rating of five at 50 days. The remaining mixes performed marginally better with moderate to severe scaling at 50 days with ratings of four (Tables 4.9 and 4.10). Taylor et al. (2004) tested the scaling resistance of samples containing either all cement, 50% slag, or 25% fly ash. They also compared the effect of different finishing techniques. They found that for samples that were finished soon after molds were filled, as was






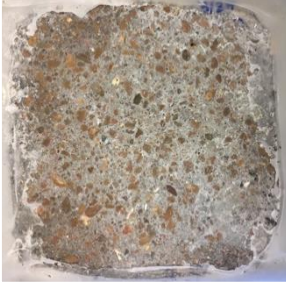




done in this study, by 50 days the all-cement samples had an average rating of 5, the 50% slag mixes had a rating of 3, and the 25% fly ash samples had a rating of 0.5.

Table 4.9 Visual rating at 50 days

Mix	Visual rating at 50 days
Control (SF8)	5
Flexural (SL22 SF8)	4
Optimal all (SL12 SF4 FA1)	5
Compressive (SL8 SF8 FA3)	4
Workability (FA31 SF4)	4

Interestingly, Bouzoubaâ et al. (2008) had different findings. Their 25-35% fly ash mixes had a 50 day rating of five, the 25-35% slag mixes had a rating of three to four, and the all-cement mix had a rating of zero. In their study, they tested seven mixes including an all-cement control, binary fly ash and slag mixes, and ternary mixes consisting of silica fume with either slag or fly ash. Similar to this study, after 50 days all mixes, excluding the all-cement mix, had ratings ranging from three to five. Sidewalks placed in Canada, which were cast from the same mixes studied, found that after four winters all mixes, but the ternary fly ash silica fume mix, had visual ratings ranging from zero to three. The ternary fly ash silica fume mix had a rating exceeding four. The authors concluded the ASTM C672 method may be too severe since the same mixes which generally performed poorly during the ASTM C672 tests performed well in the field.

Table 4.10 Deicer scaling samples before and after 50 cycles

Mix	Before (0 days)	After (50 days)
Control SF8		
Optimal flexural strength SL22 SF8		
Optimal compressive strength, flexural strength and workability SL12 SF4 FA1		
Optimal compressive strength SL8 SF8 FA3		
Optimal workability FA31 SF4		

4.3.3.3 Freeze-Thaw Resistance

Concerning freeze-thaw resistance, SL8 performed the best with a durability factor of 98.9% while SL12 SF4 FA1 and SL22 SF8 mixes performed the worst with factors of 25.1% and 30.7%, respectively (Table 4.11). The durability factor is determined using Equation 4.2 and indicates how many freeze-thaw cycles a sample can withstand before deteriorating (Toutanji et al. 2004). In particular, a durability factor of 100% after 300 cycles would mean the ultrasonic pulse velocity measured did not decrease over time, and therefore the sample has high durability during exposure to freeze-thaw cycles. A lower durability factor would demonstrate a decrease in the ultrasonic pulse velocity and subsequently lower quality and durability of the sample. It is important to keep in mind though that these factors are based on 180 cycles and not the ASTM 666 standard of 300 cycles. Therefore, all the mixes may have different durability factors than the values presented in Table 4.11.

Table 4.11 Durability factor of each mix

Mix	Durability factor (%)
Control (SF8)	98.9
Optimal Flexural (SL22 SF8)	25.1
Optimal all (SL12 SF4 FA1)	30.7
Optimal compressive (SL8 SF8 FA3)	70.1
Optimal workability (FA31 SF4)	74.2

Toutanji et al. (2004) found similar results to those presented here when they tested an all-cement mix to binary and ternary mixes of silica fume, class C fly ash and slag. The all-cement mix performed the best with a durability factor of 89.7% after 300 cycles, followed by the 8% silica fume mix at 34.9%. Overall, the binary fly ash mixes performed poorly during freeze-thaw testing while the ternary fly ash and slag mixes and the binary slag mixes had better resistance. Other research by Chung et al. (2010) on all-cement, binary 10% silica fume and binary 20% fly

ash mixes with varying w/c ratios and air contents found all mixes to have durability factors over 95%. It is important to keep in mind though that freeze-thaw laboratory cycles are more extreme than what would normally occur in the field and samples which perform poorly in the lab may not always perform poorly in the field (Mehta 1991).

4.3.3.4 Chloride Ion Penetration Resistance

All of the mixes had chloride ion permeability ratings of low (<2000 coulombs) or very low (<1000 coulombs) with the SL12 SF4 FA1 mix having the highest charge passed and the fly ash mix having the lowest (Table 4.12).

Table 4.12 Chloride permeability results

Mix	Coulombs	Rating
Control (SF8)	429	Very low
Optimal Flexural (SL22 SF8)	619	Very low
Optimal all (SL12 SF4 FA1)	1038	Low
Optimal compressive (SL8 SF8 FA3)	378	Very low
Optimal workability (FA31 SF4)	250	Very low

Gesoğlu et al. (2009) tested the chloride permeability of binary, ternary and quaternary mixes containing slag, fly ash and silica fume. While the all-cement mix had a moderate permeability rating, all the mixes containing SCMs had chloride permeability ratings of either low or very low. They also tested binary and ternary mixes similar to those tested in this study. Their data ranged from 410-800 coulombs with very low ratings, similar to the findings presented here.

Nehdi et al. (2004) tested the chloride permeability of binary mixes containing 50% fly ash or 50% slag, ternary mixes of 25% fly ash and 25% slag, and a mix containing 20% slag, 24% fly ash and 6% silica fume. The control had a high chloride ion permeability rating, the binary mixes had moderate ratings and the ternary and quaternary mixes had low permeability ratings. In a similar study Yang et al. (2017) measured the chloride permeability of all-cement mixes as well

as those containing either 40% fly ash or slag. After wet curing for five days, samples were dry cured for 360 days. The permeability ratings of the all-cement mix was moderate, the fly ash mix was low and the slag mix was very low.

CHAPTER 5.0 PRELIMINARY COST ANALYSIS

A preliminary construction cost analysis for a hypothetical mile-long two-lane high-traffic stretch of highway in Anchorage, Alaska was conducted to compare the different concrete mixes proposed. This analysis was conducted to evaluate the economic efficiency of the fix mix designs investigated. Based on material costs from Alaska Basic Industries in Anchorage from June 2019 (Schlee, 2019), the following raw material costs were assumed (Table 5.1). The cost of GGBFS in Fairbanks was assumed to be the same in Anchorage. These costs depend on availability and the market, and that if constructing a pavement on a large scale, these costs would likely be reduced due to purchasing materials in bulk.

Table 5.1 Cost of materials in Anchorage, AK in June 2019

Material	Cost per unit
silica fume	\$30 / 25-lb
fly ash	\$295 / ton
cement	\$165 /ton
GGBFS (slag)	\$250 /ton (in Fairbanks)

Using construction cost data obtained from the RS Means Heavy Construction Costs book (2019), the remaining construction costs were calculated. All costs were based on an assumed 2-lane 24-foot wide pavement with a 24-inch-thick subbase. Communications with Schaefer (2019) at Alaska DOT&PF found that a high traffic (approximately 40,000 AADT) pavement in Central Alaska would generally have an 18-36 inch deep subbase, depending on whether permafrost was present. Therefore a 24-inch thick subbase was assumed. The concrete pavement was assumed to be six inches thick with 18 pounds per square yard of reinforcing steel. In addition, transverse joint dowels were assumed to be spaced at one foot with contraction joints spaced at 12 feet. All

RS Means costs were increased by the Anchorage, Alaska rate of 115.8% the national average. In addition, following the WSDOT (2018) example calculations, cost increases of 5, 15, and 10% were added to represent mobilization, engineering, and contingencies costs, respectively (Table 5.2). The combined costs sourced from Alaska prices of cementitious materials and RS Means cost estimations resulted in the following assumed cost per two-lane one-mile stretch of pavement for each mix design (Table 5.3). These values were calculated using the assumed quantities and costs summarized in Table 5.2, but the SL8 cementitious value was changed to represent each mix's respective cementitious materials cost, which are also summarized in Table 5.3 as the cost per 6-inch-thick square-yard of pavement ($\$/6''\text{-thick}/\text{yd}^2$).

Based on the results the SL12 SF4 FA1 mix proves to be the most cost-effective design at around 1.6 million dollars. This being said, the cost between the five options varies only by about 2% with a standard deviation of \$30,000. With such a minimal difference between the construction cost of using any of the mix designs, any of them would likely be a good choice.

Since there are only a few concrete roads built and maintained by Alaska DOT&PF it is challenging to estimate and verify these costs using historical data. The cost of paving varies widely depending on the location, design, and traffic load, but for comparison, Sullivan and Moss (2014), in their report for the Portland Cement Association, estimated paving an urban 2-lane mile with concrete to cost \$770,000. Another estimate by the Arkansas Department of Transportation (ArDOT, 2016) estimates the total costs for a mile-long concrete lane in Arkansas to be \$1.1 million, or around \$2.2 per 2-lane mile. Although there appears to be a wide variance in these costs, construction costs in Alaska are likely even higher due to the geographical location and short construction season in Alaska.

Table 5.2 Assumed construction cost for 2-lane rigid pavement using Control SL8 Mix

Item	Unit	Cost /unit	Quantity /24'-wide road mile	Total (\$1000)
non-cementitious materials	6" pavement/yd ²	15.09	14080	212
SL8 cementitious materials*	6" pavement/yd ²	18.31	14080	258
placement labor and equipment	6" pavement/yd ²	4.63	14080	65
18 lb./ yd ² reinforcing steel	yd ²	15.86	14080	223
transverse joint dowels every 12'	ea.	13.32	10560	141
transverse contraction joints every 12'	l.f.	5.96	10560	63
24" deep subbase course	yd ²	31.27	14080	440
subtotal				1,403
mobilization (5% materials)			45,205	1,448
engineering and contingencies (15% mobilization and materials)			142,395	1,590
preliminary engineering (10% total)			109,169	1,699
total				1,699

*Cost/unit varies depending on mix. Cost is adjusted for Anchorage, AK prices from RS Means national average.

Table 5.3 Estimated cost of each alternative

Alternative (no.)	Cementitious Materials		Total Cost (\$/2-lane mile)
	(\$/6"-thick/yd ²)	(\$/yd ³)	
1. SF8	18.31	110	1,699,000
2. SL22 SF4	19.26	116	1,713,000
3. SL12 SF4 FA1	14.31	86	1,643,000
4. SL8 SF8 FA3	18.86	113	1,707,000
5. FA31 SF4	15.84	95	1,665,000

CHAPTER 6.0 CONCLUSIONS

The objective of this study was to identify and select concrete mix designs which would provide excellent abrasion resistance and durability. Following this a literature review of past and present studies regarding these topics was performed, as well as a survey of Alaskan engineers and Alaska DOT&PF material and pavement engineers to determine current practices and methods regarding concrete pavements in Alaska. Preliminary screening tests of ternary mixes containing silica fume with either GGBFS or class F fly ash were conducted. Tests included workability, air content, compressive strength and flexural strength. Following this four optimal mixes were determined using the statistical software Minitab. Results obtained were verified using special cubic models and desirability functions. These four mixes, as well as the control binary mix, were then subjected to further durability and mechanical testing. These mixes included an 8% silica fume control mix (SF8), a 22% slag with 8% silica fume mix (SL22 SF8), 12% slag with 4% silica fume and 1% fly ash mix (SL12 SF4 FA1), 8% slag with 8% silica fume and 3% fly ash mix (SL8 SF8 FA3) and a mix containing 31% fly ash with 4% silica fume (FA31 SF4). Testing included drying shrinkage, abrasion resistance, scaling resistance to deicer salts, F-T resistance and chloride ion penetration resistance. Regarding each test the following results were found:

- Regarding compressive strength and shrinkage, by 28 days the SF8 had the highest compressive strength while the FA31 SF4 mix had the lowest drying shrinkage at 0.01% expansion. However, all mixes have 28-day compressive strength greater than 6,000 psi, which fulfills the minimum strength requirement of 6,000 psi to be considered high-strength

concrete (ACI, 1992). All mixes are also within the SCM drying shrinkage limits of 0.04% suggested by Mokarem et al. (2005).

- For abrasion resistance the FA31 SF4 mix had the highest resistance by mass loss and the SL12 SF4 FA1 mix had the lowest volumetric mass loss by Prall abrasion testing. Regarding the mass loss, an average of only one gram of material was lost after each application of the drill press, so overall there was almost negligible mass loss equivalent to 0.01-0.03% per sample, indicative of likely a high abrasion resistance to studded tires. For Prall abrasion testing, two mixes had Nordic Classifications of satisfactory while the remaining three were classified as less satisfactory. Although the classification ratings are not all satisfactory, it is important to keep in mind this test is usually used for asphalt pavements, and other researchers (i.e. Scholz and Keshari, 2010) which used Prall testing to test their 8,000 psi concrete found their ratings to be classified as less satisfactory as well, similar to these findings.
- The SL22 SF8, SL8 SF8 FA3 and FA31 SF4 mixes had similar 50 day visual ratings of four, equivalent to moderate to severe scaling, when measuring their respective deicer salt scaling resistance. The SL8 SF8 FA3 and SL12 SF4 FA1 mixes performed worse with visual ratings of five, equivalent to severe scaling. Although these ratings indicate the samples performed poorly, this may not be indicative of field performance. For example, Bouzoubaâ et al. (2008) found that SCM mixes which performed poorly during ASTM C672 did not have as severe scaling in the field.
- After testing chloride ion penetration, all mixes but SL12 SF4 FA1 had very low ratings of less than 1,000 coulombs. SL12 SF4 FA1 had a low rating of 1,038 coulombs. FA31 SF4 had

the lowest rating of 250 coulombs. Therefore all the mixes likely have low permeability and subsequently high durability.

- For F-T resistance after 180 cycles the SF8 mix performed the best with a durability factor of 99% while the SL22 SF8 and SL12 SF4 FA1 mixes performed the worst with durability factors of 25% and 31%, respectively. The other two had factors of 70% and 74%. A durability factor below 60% is considered failure, at which point testing can end, and by 180 cycles two of the five mixes had failed. A preliminary cost analysis comparing the construction costs in Alaska associated with each of the five performance testing mixes found that the SL12 SF4 FA1 mix would have the lowest construction cost of \$1.6 million per 2-lane highway. The variance in cost though was minimal with the construction costs of the five mixes ranging from \$1.6 to \$1.7 million.

In terms of the properties evaluated within this study (i.e. strength, shrinkage, chloride ion penetration, F-T resistance, deicer scaling resistance, and abrasion resistance), the five mixes, including the four optimal mixes and control, all provided overall good performance. Therefore of the five mixes, the quaternary SL12 SF4 FA1 provided the overall best performance due to its good strength and abrasion resistance, favorable fresh and durability properties, and low construction cost. Subsequently, within the scope of this study, a quaternary mix design, containing primarily silica fume and slag, appears to provide the overall best performance in terms of strength, durability, abrasion resistance, and cost.

The next recommended step in this research would be constructing and monitoring test sections in the field using the optimal mixes determined to verify and validate results generated from the

laboratory tests. Long-term performance data could be collected and analyzed for an in-depth life cycle cost analysis. In addition, this study focused on silica fume, slag, and fly ash, but further research could investigate other types and dosages of SCMs using additional tests and more extensive F-T testing. Additionally, these tests primarily focused on properties measured over 28 days and longer term strength and durability properties were not investigated. Further research into the long term durability characteristics of abrasion resistant concrete pavements would also be beneficial.

CHAPTER 7.0 REFERENCES

- AASHTO (2017). TP 118-17 "Standard Method of Test for Characterization of the Air-Void System of Freshly Mixed Concrete by the Sequential Pressure Method." Washington, D.C.: AASHTO.
- Abdun-Nur, E. A. (1961). "Fly Ash in Concrete, an Evaluation-Annotated Bibliograph." Highway research board bulletin (284).
- "Abrasion by Studs, Method A: Prall Method." CEN WG1 Bituminous Materials, European Standard Working Draft, Testing Bituminous Materials, TG2, Reference No.: 1.14, TC 227, Work Item 00227122, Second Draft, March 1997.
- ACI (2011). "233R-03: Slag Cement in Concrete and Mortar." Technical Documents. American Concrete Institute. Farmington Hills, MI.
- ACI. (2012). "234R-06: Guide for the Use of Silica Fume in Concrete." Technical Documents. American Concrete Institute. Farmington Hills, MI.
- AFCESA/CES. (2001). Engineering Technical Letter (ETL) 01-8: Resin Modified Pavement (RMP) Design and Application Criteria Tyndall AFB, FL.
- Alaska DOT&PF (2017). "Standard Specifications for Highway Construction." Alaska Department of Transportation and Public Facilities. Juneau, AK.
- Alaska DOT&PF (2018). "Atigun River No. 2 Bridge on Dalton Highway." Alaska Department of Transportation and Public Facilities Bridge Section.
- Alaska DOT&PF (2018). "Troublesome Creek Bridge Deck." Department of Transportation and Public Facilities Bridge Section.
- "Alaska DOT&PF Regions." (n.d.). Alaska Department of Transportation and Public Facilities. Retrieved from <http://dot.alaska.gov/regions-portal.shtml>.
- Akkaya, Y., Ouyang, C., & Shah, S. P. (2007). "Effect of supplementary cementitious materials on shrinkage and crack development in concrete." *Cement and Concrete Composites*, 29(2), 117-123.
- Aksezer, C. S. (2008). "On the sensitivity of desirability functions for multiresponse optimization." *Journal of Industrial and Management Optimization*, 4(4), 685-696.
- Anderson, K. W., Uhlmeyer, J. S., Russell, M., & Weston, J. (2011). "Studded tire wear resistance of PCC pavements with special mix design: contract 6620, I-90, Argonne Road to Sullivan Road, MP 286.91 to 292.38 (No. WA-RD 658.2)." Washington State Department of Transportation.

- Anderson, K. W., Uhlmeier, J., & Russell, M. (2009). "Combined Aggregate Gradation as a Method for Mitigating Studded Tire Wear on PCCP (No. WA-RD 663.2)." Washington State Department of Transportation.
- Anderson, K. W., Uhlmeier, J. S., & Pierce, L. (2007). "Studded Tire Wear Resistance of PCC Pavements (No. WA-RD 658.1)." Washington State Department of Transportation.
- Angerinos, M. J., Mahoney, J. P., Moore, R. L., & O'Brien, A. J. (1999). "A Synthesis on Studded Tires." Washington State Transportation Center (TRAC). Report No. WARD, 471, 52.
- ArDOT (2016). "Estimated Costs per Mile." Retrieved from [https://www.arkansashighways.com/roadway_design_division/Cost%20per%20Mile%20\(JULY%202016\).pdf](https://www.arkansashighways.com/roadway_design_division/Cost%20per%20Mile%20(JULY%202016).pdf)
- ASTM. (2012a). "ASTM C672/C672M-12 Standard Test Method for Scaling Resistance of Concrete Surfaces Exposed to Deicing Chemicals." West Conshohocken, PA: ASTM International.
- ASTM. (2012b). "ASTM C944/C944M-12 Standard Test Method for Abrasion Resistance of Concrete or Mortar Surfaces by the Rotating-Cutter Method." West Conshohocken, PA: ASTM International.
- ASTM. (2015a). "ASTM C143/C143M-15a Standard Test Method for Slump of Hydraulic-Cement Concrete." West Conshohocken, PA: ASTM International.
- ASTM. (2015b). "ASTM C666/C666M-15 Standard Test Method for Resistance of Concrete to Rapid Freezing and Thawing." West Conshohocken, PA: ASTM International.
- ASTM. (2017a). "ASTM C157/C157M-17 Standard Test Method for Length Change of Hardened Hydraulic-Cement Mortar and Concrete." West Conshohocken, PA: ASTM International.
- ASTM. (2017b). "ASTM C231/C231M-17a Standard Test Method for Air Content of Freshly Mixed Concrete by the Pressure Method." West Conshohocken, PA: West Conshohocken, PA.
- ASTM (2018). "ASTM C39/C39M-18 Standard Test Method for Compressive Strength of Cylindrical Concrete Specimens." West Conshohocken, PA: West Conshohocken, PA.
- ASTM. (2019). "ASTM C1202-19 Standard Test Method for Electrical Indication of Concrete's Ability to Resist Chloride Ion Penetration." West Conshohocken, PA: ASTM International.

- Atiş, C. D. (2002). "High volume fly ash abrasion resistant concrete." *Journal of Materials in Civil Engineering*, 14(3), 274-277.
- Babashamsi, P., Md Yusoff, N. I., Ceylan, H., Md Nor, N. G., & Salarzadeh Jenatabadi, H. (2016). "Evaluation of pavement life cycle cost analysis: Review and analysis." *International Journal of Pavement Research and Technology*, 9(4), 241-254.
- Badr, A. (2010). "Freeze-thaw durability of Portland cement and silica fume concretes." Paper presented at the Sixth International Conference on Concrete under Severe Conditions: Environment and Loading.
- Batthey, R. L., & Whittington, J. S. (2007). "Construction, Testing and Performance Report on the Resin Modified Pavement Demonstration Project." (No. FHWA/MS-DOT-RD-07-137).
- Berndt, M. (2009). "Properties of sustainable concrete containing fly ash, slag and recycled concrete aggregate." *Construction and Building Materials*, 23(7), 2606-2613.
- Bhanja, S., & Sengupta, B. (2005). "Influence of silica fume on the tensile strength of concrete." *Cement and Concrete Research*, 35(4), 743-747.
- Bharatkumar, B., Narayanan, R., Raghuprasad, B., & Ramachandramurthy, D. (2001). "Mix proportioning of high performance concrete." *Cement and Concrete Composites*, 23(1), 71-80.
- Bleszynski, R., Hooton, R. D., Thomas, M. D., & Rogers, C. A. (2002). "Durability of ternary blend concrete with silica fume and blast-furnace slag: laboratory and outdoor exposure site studies." *Materials Journal*, 99(5), 499-508.
- Bouzoubaâ, N., Bilodeau, A., Fournier, B., Hooton, R., Gagné, R., & Jolin, M. (2008). "Deicing salt scaling resistance of concrete incorporating supplementary cementing materials: laboratory and field test data." *Canadian Journal of Civil Engineering*, 35(11), 1261-1275.
- Bowthorpe, T., Southcoast Region Materials Lab, Alaska DOT&PF (2019). Personal communication.
- Brunette, B., Retired Materials Engineer, Alaska DOT&PF (2019). Personal communication.
- Chung, C.-W., Shon, C.-S., & Kim, Y.-S. (2010). "Chloride ion diffusivity of fly ash and silica fume concretes exposed to freeze-thaw cycles." *Construction and Building Materials*, 24(9), 1739-1745.
- Connor, B., Alaska University Transportation Center Director, University of Alaska Fairbanks (2019). Personal communication.

- Cotter, A., & Muench, S. T. (2010). "Studded tire wear on Portland cement concrete pavement in the Washington State Department of Transportation route network." (No. WA-RD 744.3). Washington State Department of Transportation. Office of Research and Library Services.
- Currey, J., Northern Regions Materials Engineer, Alaska DOT&PF (2018). Personal interview with X. Schlee.
- Davis, R. E., Carlson, R. W., Kelly, J. W., & Davis, H. E. (1937). "Properties of cements and concretes containing fly ash." Paper presented at the Journal Proceedings.
- Derringer, G., & Suich, R. (1980). "Simultaneous optimization of several response variables." *Journal of quality technology*, 12(4), 214-219.
- Detwiler, R. J., & Mehta, P. K. (1989). "Chemical and physical effects of silica fume on the mechanical behavior of concrete." *Materials Journal*, 86(6), 609-614.
- El-Chabib, H., & Syed, A. (2012). "Properties of self-consolidating concrete made with high volumes of supplementary cementitious materials." *Journal of Materials in Civil Engineering*, 25(11), 1579-1586.
- Erdem, T. K., & Kırca, Ö. (2008). "Use of binary and ternary blends in high strength concrete." *Construction and Building Materials*, 22(7), 1477-1483.
- Fernandez, L., & Malhotra, V. M. (1990). "Mechanical properties, abrasion resistance, and chloride permeability of concrete incorporating granulated blast-furnace slag." *Cement, concrete and aggregates*, 12(2), 87-100.
- FHWA. (2018). "Functional System Length - 2018. Miles by type of surface - rural." Federal Highway Association.
- Fidjestel, P., Luther, M., Danielssen, T., Obuchowicz, M., & Tutokey, S. (1989). "Silica fume-efficiency versus form of delivery." Paper presented at the Proceedings of the 3rd international conference on the use of fly ash slag, silica fume and natural pozzolans in concrete, Trondheim (supplementary papers volume).
- Gartin, R. S., & Saboundjian, S. (2005). "Development and Validation of Urban Alaskan Pavement Rutting Models." (No. FHWA-AK-RD-04-02).
- Gesoğlu, M., Güneyisi, E., & Özbay, E. (2009). "Properties of self-compacting concretes made with binary, ternary, and quaternary cementitious blends of fly ash, blast furnace slag, and silica fume." *Construction and Building Materials*, 23(5), 1847-1854.
- Ghafoori, N., & Diawara, H. (1999). "Abrasion resistance of fine aggregate-replaced silica fume concrete." *Materials Journal*, 96(5), 559-569.

- Grdic, Z. J., Curcic, G. A. T., Ristic, N. S., & Despotovic, I. M. (2012). "Abrasion resistance of concrete micro-reinforced with polypropylene fibers." *Construction and Building Materials*, 27(1), 305-312.
- Güneyisi, E., Gesoğlu, M., Karaoğlu, S., & Mermerdaş, K. (2012). "Strength, permeability and shrinkage cracking of silica fume and metakaolin concretes." *Construction and Building Materials*, 34, 120-130.
- Hagerman, K., Former Public Works Director, Borough of Petersburg, Alaska (2019). Personal communication.
- Hale, W. M., Freyne, S. F., Bush Jr, T. D., & Russell, B. W. (2008). "Properties of concrete mixtures containing slag cement and fly ash for use in transportation structures." *Construction and Building Materials*, 22(9), 1990-2000.
- Hamilton, H. R., Nash, T., Van Etten, N., & Vivas, E. (2009). "Durability and mechanical properties of ternary blend concretes (No. 50495)." University of Florida. Dept. of Civil and Coastal Engineering.
- Harai, S., Senior Engineer, Harai & Associates, Inc. (2019). Personal communication.
- Harings, D., Northwest Region Pavement Engineer, Wisconsin DOT (2019). Personal communication.
- Hilson, M., Public Works Director, Ketchikan, Alaska (2019). Personal communication.
- Hobbs, D. (2001). "Concrete deterioration: causes, diagnosis, and minimising risk." *International Materials Reviews*, 46(3), 117-144.
- Hooton, R. D. (2000). "Canadian use of ground granulated blast-furnace slag as a supplementary cementing material for enhanced performance of concrete." *Canadian Journal of Civil Engineering*, 27(4), 754-760.
- Hossain, A. B., Shrestha, S., & Summers, J. (2009). "Properties of concrete incorporating ultrafine fly ash and silica fume." *Transportation Research Record*, 2113(1), 41-46.
- Howell, R., Public Works Director, Wrangell, Alaska (2019). Personal communication.
- Janotka, I. (2007). "Durability of High-Strength Concrete with Silica Fume: Temperature Attack and Freezing-and-Thawing Cycles." *Special Publication*, 242, 175-186.
- Johnson, D. Anchorage Sand & Gravel. (2019) Personal communication.

- Juenger, M. C., & Siddique, R. (2015). "Recent advances in understanding the role of supplementary cementitious materials in concrete." *Cement and Concrete Research*, 78, 71-80.
- Justnes, H. (2007). "Silica Fume in High-Quality Concrete--A Review of Mechanism and Performance." *Special Publication*, 242, 63-78.
- Kabay, N. (2014). "Abrasion resistance and fracture energy of concretes with basalt fiber." *Construction and Building Materials*, 50, 95-101.
- Kemp, P., Pavement Unit Supervisor, Wisconsin DOT (2019). Personal communication.
- Keyser, J. H. (1971). "Resistance of Various Types of Bituminous Concrete and Cement Concrete to Wear by Studded Tires." *Highway Research Record* (352).
- Kuennen, T. (2004). "America's Quest for Premium Aggregates." *Better Roads*, 74(8).
- Langan, B., Joshi, R., & Ward, M. (1990). "Strength and durability of concretes containing 50% Portland cement replacement by fly ash and other materials." *Canadian Journal of Civil Engineering*, 17(1), 19-27.
- Lee, J.-H., & Yoon, Y.-S. (2015). "The effects of cementitious materials on the mechanical and durability performance of high-strength concrete." *KSCE Journal of Civil Engineering*, 19(5), 1396-1404.
- Li, H., Zhang, M.-h., & Ou, J.-p. (2006). "Abrasion resistance of concrete containing nanoparticles for pavement." *Wear*, 260(11-12), 1262-1266.
- Lothenbach, B., Scrivener, K., & Hooton, R. (2011). "Supplementary cementitious materials." *Cement and Concrete Research*, 41(12), 1244-1256.
- Lundy, J. R., Hicks, R. G., Scholz, T. V., & Esch, D. C. (1992). "Wheel track rutting due to studded tires." *Transportation Research Record*, 18-18.
- Mack, S. (2010). "H.C. Redi Mix 65341 for Tok Weigh Station Report for AK DOT Northern Region." Mappa Inc.
- Malik, M. G. (2000). "Studded Tires in Oregon: Analysis of Pavement Wear and Cost of Mitigation." Financial and Economic Analysis Unit, Financial Services, Central Services Division, Oregon Department of Transportation.
- Mappa, Inc. (2018). "Aggregate Service Record Twin Rich Pit, North Pole, AK Report for University Redi Mix Concrete Products."
- Marx, E., Senior Bridge Engineer, Alaska DOT&PF (2019). Personal communication.

- Masad, E., & James, L. (2001). "Implementation of high performance concrete in Washington State (No. WA-RD 530.1.)."
- Mazloom, M., Ramezani-pour, A., & Brooks, J. (2004). "Effect of silica fume on mechanical properties of high-strength concrete." *Cement and Concrete Composites*, 26(4), 347-357.
- Mehta, P. K. "Durability of Concrete--Fifty Years of Progress?" ACI Symposium Publication, 126.
- Meusel, J., & Rose, J. (1983). "Production of granulated blast furnace slag at sparrows point, and the workability and strength potential of concrete incorporating the slag." Special Publication, 79, 867-890.
- Miller, J. S., & Bellinger, W. Y. (2014). "Distress identification manual for the long-term pavement performance program (No. FHWA-HRT-13-092)." United States. Federal Highway Administration. Office of Infrastructure Research and Development.
- Minitab 19 Statistical Software (2019). [Computer software]. State College, PA: Minitab, Inc. (www.minitab.com)
- Mokarem, D. W., Weyers, R. E., & Lane, D. S. (2005). "Development of a shrinkage performance specifications and prediction model analysis for supplemental cementitious material concrete mixtures." *Cement and Concrete Research*, 35(5), 918-925.
- Naik, T. R., & Ramme, B. W. (1989). "High early strength concrete containing large quantities of fly ash." *ACI materials journal*, 86(2), 111-116.
- Nehdi, M., Pardhan, M., & Koshowski, S. (2004). "Durability of self-consolidating concrete incorporating high-volume replacement composite cements." *Cement and Concrete Research*, 34(11), 2103-2112.
- Niemi, A. (1978). "Technical Raid Studies Related to Studded Tires." Proc., Road Paving Research, Helsinki University of Technology, Finland, 25-33.
- Obla, K. H., Hill, R. L., Thomas, M. D., Shashiprakash, S. G., & Perebatova, O. (2003). "Properties of concrete containing ultra-fine fly ash." *ACI materials journal*, 100(5), 426-433.
- ODOT (1974). "The Use and Effects of Studded Tires in Oregon." Oregon Department of Transportation. Salem, OR.

- Oner, A., Akyuz, S., & Yildiz, R. (2005). "An experimental study on strength development of concrete containing fly ash and optimum usage of fly ash in concrete." *Cement and Concrete Research*, 35(6), 1165-1171.
- Osborne, G. (1999). "Durability of Portland blast-furnace slag cement concrete." *Cement and Concrete Composites*, 21(1), 11-21.
- Radlinski, M., Olek, J., & Nantung, T. (2008). "Effect of mixture composition and initial curing conditions on scaling resistance of ternary (OPC/FA/SF) concrete." *Journal of Materials in Civil Engineering*, 20(10), 668-677.
- Ramana, G., Potharaju, V., Mahure, M., & Ratnam, M. (2014). "Abrasion Resistance of Multi Blended Concrete Mixes Containing Fly Ash and Silica Fume." *International Journal of Engineering Science and Technology*, 6(6), 338.
- Rashad, A. M., Seleem, H. E.-D. H., & Shaheen, A. F. (2014). "Effect of Silica Fume and Slag on Compressive Strength and Abrasion Resistance of HVFA Concrete." *International Journal of Concrete Structures and Materials*, 8(1), 69-81.
- Ravina, D., & Mehta, P. K. (1986). "Properties of fresh concrete containing large amounts of fly ash." *Cement and Concrete Research*, 16(2), 227-238.
- RSMeans (2019). "Heavy construction costs with RSMeans data 2019." Norwell, MA: RSMeans.
- Rupnow, T. D. (2012). "Evaluation of ternary cementitious combinations (No. FHWA/LA. 11/486)." Louisiana Transportation Research Center.
- san Angelo, M., Statewide Materials Engineer, Alaska DOT&PF (2019). Personal Communication.
- Schaefer, H., Northern Regions Materials Lab Supervisor, Alaska DOT&PF (2019). Personal communication.
- Schlee, X., Alaska Concrete Alliance Co-Chair, Alaska Basic Industries Technical Sales (2019). Personal communications.
- Schlroholtz, S. (2004). "Development of performance of ternary mixes: Scoping study." Rep. No. DTFH61-01-X-00042 (Project 13), Center for Portland Cement Concrete Pavement Technology, Ames, IA.
- Scholz, T. V., & Keshari, S. (2010). "Abrasion-resistant concrete mix designs for precast bridge deck panels (No. FHWA-OR-RD-11-04)." Kiewit Center for Infrastructure and Transportation.

- Shannag, M. (2000). "High strength concrete containing natural pozzolan and silica fume." *Cement and Concrete Composites*, 22(6), 399-406.
- Shehata, M. H., & Thomas, M. D. (2002). "Use of ternary blends containing silica fume and fly ash to suppress expansion due to alkali-silica reaction in concrete." *Cement and Concrete Research*, 32(3), 341-349.
- Shippen, N., Kennedy, M., & Pennington, L. S. (2014). "Review of Studded Tires in Oregon (No. FHWA-OR-RD-15-07)."
- Sivasundaram, V., & Malhotra, V. (1992). "Properties of concrete incorporating low quantity of cement and high volumes of ground granulated slag." *Materials Journal*, 89(6), 554-563.
- Sonafrank, C. (2010). "Investigating 21st century cement production in interior Alaska using Alaskan resources." Cold Climate Housing Research Center, Report, 12409.
- "Statewide Socioeconomic Impacts of Usibelli Coal Mine, Inc." (2015). McDowell Group. Prepared for Usibelli Coal Mine, Inc. Retrieved from <http://www.usibelli.com/pdf/McDowell-Report-Statewide-Socioeconomic-Impacts-of-UCM-2015l.pdf>
- Sullivan, E and Moss, A (2014). *Paving Cost Comparisons: Warm-Mix Asphalt Versus Concrete*. Portland Cement Association Market Intelligence.
- Sutter, L. L. (2016). "Supplementary Cementitious Materials-Best Practices for Concrete Pavements:[techbrief] (No. FHWA-HIF-16-001). United States. Federal Highway Administration.
- Taylor, P. C., Morrison, W., & Jennings, V. A. (2004). "Effect of Finishing Practices on Performance of Concrete Containing Slag and Fly Ash as Measured by ASTM C 672 Resistance to Deicer Scaling Tests." *Cement, concrete and aggregates*, 26(2), 1-5.
- Thomas, M., Hopkins, D. S., Perreault, M., & Cail, K. (2007). "Ternary cement in Canada." *Concrete international*, 29(7), 59-64.
- Thomas, M., Shehata, M., Shashiprakash, S., Hopkins, D., & Cail, K. (1999). "Use of ternary cementitious systems containing silica fume and fly ash in concrete." *Cement and Concrete Research*, 29(8), 1207-1214.
- Toutanji, H., Delatte, N., Aggoun, S., Duval, R., & Danson, A. (2004). "Effect of supplementary cementitious materials on the compressive strength and durability of short-term cured concrete." *Cement and Concrete Research*, 34(2), 311-319.

- Turk, K., & Karatas, M. (2011). "Abrasion resistance and mechanical properties of self-compacting concrete with different dosages of fly ash/silica fume." *Indian Journal of Engineering and Materials Sciences*, 18, 49–60.
- Van Dam, E. (2014). "Abrasion resistance of concrete and the use of high performance concrete for concrete railway crossties" (Masters thesis, University of Illinois at Urbana-Champaign).
- Wang, F. H., & Li, S. (2012). "Effect of silica fume on workability and water impermeability of concrete." Paper presented at the Applied Mechanics and Materials.
- Wisconsin State Legislature. (2017). "Chapter 347.45 Tire equipment." Retrieved from <https://docs.legis.wisconsin.gov/statutes/statutes/347/III/45>.
- Won, M. C., Kim, S.-M., Merritt, D., & McCullough, B. F. (2002). "Horizontal cracking and pavement distress in Portland cement concrete pavement." *Designing, Constructing, Maintaining, and Financing Today's Airport Projects* (pp. 1-10).
- Wongkeo, W., Thongsanitgarn, P., Ngamjarurojana, A., & Chaipanich, A. (2014). "Compressive strength and chloride resistance of self-compacting concrete containing high level fly ash and silica fume." *Materials & Design*, 64, 261-269.
- WSDOT. (2006). "Pavements and Studded Tire Damage." Washington State Department of Transportation. State Materials Laboratory. Retrieved from <https://www.wsdot.wa.gov/NR/rdonlyres/098E61DC-AD06-486D-AFA2-808207BCEE7E/0/PavementsStuddedTires.pdf>
- WSDOT. (2016). "Technical Brief: Estimate of Annual Studded Tire Damage to Concrete Pavements." Washington State Department of Transportation. Construction Division. State Materials Lab.
- WSDOT (2018). "Pavement Policy." Washington State Department of Transportation. Multimodal Development and Delivery. Pavement Office. Olympia, WA.
- Yang, J., Wang, Q., & Zhou, Y. (2017). "Influence of curing time on the drying shrinkage of concretes with different binders and water-to-binder ratios." *Advances in Materials Science and Engineering*, 2017.
- Yen, T., Hsu, T.-H., Liu, Y.-W., & Chen, S.-H. (2007). "Influence of class F fly ash on the abrasion–erosion resistance of high-strength concrete." *Construction and Building Materials*, 21(2), 458-463.
- Yener, E., & Hınısliođlu, S. (2011). "The effects of silica fume and fly ash on the scaling resistance and flexural strength of pavement concretes." *Road Materials and Pavement Design*, 12(1), 177-194.

Yogendran, V., Langan, B., Haque, M., & Ward, M. (1987). "Silica fume in high-strength concrete." *Materials Journal*, 84(2), 124-129.

Zubeck, H., Aleshire, L., Harvey, S., Porhola, S., & Larson, E. (2004). "Socio-Economic Effects of Studded Tire Use in Alaska." Final Report. University of Alaska Anchorage, 156.

APPENDIX

Table A-1 Alaska fine aggregate gradation

Sieve No.	% Total	% Passing
1/2"	0.02	99.98
3/8"	0.01	99.97
#4	0.88	99.09
#8	8.23	90.86
#16	19.63	71.23
#30	43.71	27.52
#50	19.25	8.26
#100	6.53	1.73

Table A-2 Alaska intermediate aggregate gradation

Sieve No.	% Total	% Passing
1/2"	0.03	99.97
3/8"	1.74	98.23
#4	94.09	4.14
#8	3.81	0.33
#16	0.27	0.06
#30	0.01	0.05
#50	0.02	0.03
#100	0.00	0.03

Table A-3 Missouri fine aggregate gradation

Sieve No.	% Total	% Passing
3/4"	0.00	100.00
3/8"	0.06	100.00
#4	-0.01	100.00
#8	19.48	80.52
#16	11.53	68.99
#30	29.82	39.16
#50	29.52	9.65
#100	9.59	0.05

Table A-4 Missouri intermediate aggregate gradation

Sieve No.	% Total	% Passing
3/4"	0.00	100.00
3/8"	1.56	98.44
#4	82.67	15.77
#8	14.91	0.86
#16	0.56	0.29
#30	0.15	0.15
#50	0.15	0.00
#100	0.00	0.00

Table A-5 Prall test results

DEPARTMENT OF TRANSPORTATION SOUTHEAST MATERIALS LAB PRALL WORKSHEET							
PROJECT: Diane Murph/Jenny Liu Research project					SAMPLE DATE: <u>6/7/2019</u> TECH: <u>TB</u>		
Sample Number	Mass in Air (A)	Weight in Water (B)	Mass SSD (C)	Bulk Spg. Grav. A/(C-B)	Mass Cold before Abras. SSD	Mass after Abras. SSD	Abrasion Value
1a	599.0	349.0	600.5	2.382	582.8	475.6	45.0
1b	571.8	333.9	573.0	2.391	574.6	465.7	45.5
						Average	45.3
2a	585.1	343.8	586.5	2.411	587.7	471.9	48.0
2b	604.8	352.9	606.4	2.386	583.8	492.5	38.3
						Average	43.2
3a	550.6	313.8	552.8	2.304	555.7	460.6	41.3
3b	569.1	322.9	571.5	2.289	545.0	468.9	33.2
						Average	37.3
4a	557.3	315.9	559.9	2.284	532.7	449.3	36.5
4b	545.2	311.1	548.0	2.301	551.1	453.6	42.4
						Average	39.4
5a	517.3	288.9	520.1	2.237	524.6	419.5	47.0
5b	569.3	321.0	572.4	2.265	551.5	433.7	52.0
						Average	49.5